

This article was downloaded by: [Felipe Chinaglia Montefeltro]

On: 08 January 2013, At: 08:52

Publisher: Taylor & Francis

Informa Ltd Registered in England and Wales Registered Number: 1072954 Registered office: Mortimer House, 37-41 Mortimer Street, London W1T 3JH, UK



Journal of Vertebrate Paleontology

Publication details, including instructions for authors and subscription information:

<http://www.tandfonline.com/loi/ujvp20>

Postcranial anatomy of the hyperodapedontine rhynchosaur *Teyumbaita sulcognathus* (Azevedo and Schultz, 1987) from the Late Triassic of Southern Brazil

Felipe Chinaglia Montefeltro ^a, Jonathas Souza Bittencourt ^b, Max Cardoso Langer ^a & Cesar Leandro Schultz ^c

^a Laboratório de Paleontologia, Departamento de Biologia, Faculdade de Filosofia, Ciências e Letras de Ribeirão Preto, Universidade de São Paulo, Av. Bandeirantes 3900, 14040-901, Ribeirão Preto SP, Brazil

^b Departamento de Geologia, Instituto de Geociências, Universidade Federal de Minas Gerais, Av. Antônio Carlos 6.627, Pampulha, 31270-901, Belo Horizontem MG, Brazil

^c Departamento de Paleontologia e Estratigrafia, Universidade Federal do Rio Grande do Sul, Av. Bento Gonçalves 9500, 91540-000, Porto Alegre RS, Brazil

To cite this article: Felipe Chinaglia Montefeltro, Jonathas Souza Bittencourt, Max Cardoso Langer & Cesar Leandro Schultz (2013): Postcranial anatomy of the hyperodapedontine rhynchosaur *Teyumbaita sulcognathus* (Azevedo and Schultz, 1987) from the Late Triassic of Southern Brazil, *Journal of Vertebrate Paleontology*, 33:1, 67-84

To link to this article: <http://dx.doi.org/10.1080/02724634.2012.710285>

PLEASE SCROLL DOWN FOR ARTICLE

Full terms and conditions of use: <http://www.tandfonline.com/page/terms-and-conditions>

This article may be used for research, teaching, and private study purposes. Any substantial or systematic reproduction, redistribution, reselling, loan, sub-licensing, systematic supply, or distribution in any form to anyone is expressly forbidden.

The publisher does not give any warranty express or implied or make any representation that the contents will be complete or accurate or up to date. The accuracy of any instructions, formulae, and drug doses should be independently verified with primary sources. The publisher shall not be liable for any loss, actions, claims, proceedings, demand, or costs or damages whatsoever or howsoever caused arising directly or indirectly in connection with or arising out of the use of this material.

POSTCRANIAL ANATOMY OF THE HYPERODAPEDONTINE RHYNCHOSAUR
TEYUMBAITA SULCOGNATHUS (AZEVEDO AND SCHULTZ, 1987) FROM THE LATE
TRIASSIC OF SOUTHERN BRAZIL

FELIPE CHINAGLIA MONTEFELTRO,^{*1} JONATHAS SOUZA BITTENCOURT,² MAX CARDOSO LANGER,¹
and CESAR LEANDRO SCHULTZ³

¹Laboratório de Paleontologia, Departamento de Biologia, Faculdade de Filosofia, Ciências e Letras de Ribeirão Preto, Universidade de São Paulo, Av. Bandeirantes 3900, 14040-901, Ribeirão Preto SP, Brazil, felipecm@pg.ffclrp.usp.br; mclanger@ffclrp.usp.br;

²Departamento de Geologia, Instituto de Geociências, Universidade Federal de Minas Gerais, Av. Antônio Carlos 6.627, Pampulha, 31270-901, Belo Horizonte MG, Brazil, sigmaorionis@yahoo.com.br;

³Departamento de Paleontologia e Estratigrafia, Universidade Federal do Rio Grande do Sul, Av. Bento Gonçalves 9500, 91540-000 Porto Alegre RS, Brazil, cesar.schultz@ufrgs.br

ABSTRACT—*Teyumbaita sulcognathus* is a peculiar endemic Brazilian rhynchosaur that remained somewhat obscure until recently, when its skull anatomy was described and a new generic name was assigned to this highly autapomorphic taxon. Here, the postcranial skeleton of *Teyumbaita sulcognathus* is for the first time fully described based on the holotype and the two more complete referred specimens. Rhynchosaur postcranial anatomy has usually been considered to be rather conservative, but *T. sulcognathus* shows unforeseen morphological variation. Autapomorphic traits were added to the diagnosis of *T. sulcognathus* and intraspecific variation was also identified. In addition, six new phylogenetically informative postcranial characters were recognized. Some of these represent apomorphies of clades such as Rhynchosauridae (axis with ventral keel, crest on the anteromedial surface of tibial shaft) and Hyperodapedontinae (postaxial cervical vertebrae with ventral keel, supinator process composed of a low supinator ridge and the ligament groove), revealing new support for their monophyly. The rhynchosaur diversity of the Otter Sandstone Formation (England) was also evaluated based on a phylogenetic analysis. The results suggest that the postcranium EXEMS 79/1992 is more likely related to *Fodonyx spenceri* than to *Bentonyx sidensis*.

SUPPLEMENTAL DATA—Supplemental materials are available for this article for free at www.tandfonline.com/UJVP

INTRODUCTION

Teyumbaita sulcognathus was originally described by Azevedo and Schultz (1987) as *Scaphonyx sulcognathus*, and later transferred to a new genus by Montefeltro et al. (2010), based on a set of cranial autapomorphies that emphasized its highly modified morphology. The few postcranial elements of its holotype (UFRGS-PV-0232T) were described by Schultz (1986), but the skeleton has since been further prepared. Coupled with the recovery of additional specimens (UFRGS-PV-0290T, UFRGS-PV-0298T), this increased the amount of postcranial material available for the taxon, leading to the following description.

The rhynchosaur postcranium has historically been relegated to a secondary source of information in comparison with cranial and dental structures (Benton, 1983; Langer and Schultz, 2000; Langer et al., 2000a; Nesbitt and Whatley, 2004). This is also true for phylogenetic analyses, which usually rely on a small number of postcranial characters; for example, Hone and Benton (2008) and Langer et al. (2010) included only 24 (out of a total of 75) and 11 (out of a total of 59) postcranial characters in their analyses, respectively.

The aim of the present paper is to redescribe the postcranial material of *T. sulcognathus*, comparing the postcranium of this endemic Brazilian hyperodapedontine with other rhynchosaur taxa, in order to recognize autapomorphic features and useful characters for phylogenetic analyses. We also conducted an

exploratory analysis aiming at a better understanding of the rhynchosaur diversity of the Anisian-aged Otter Sandstone Formation (Devon, England).

Institutional Abbreviations—**BRSUG**, Bristol University, Department of Geology, Bristol, U.K.; **EXEMS**, Royal Albert Museum, Exeter, U.K.; **FZB-PV**, Fundação Zoobotânica do Rio Grande do Sul, Porto Alegre, Brazil; **IGMPT**, Institut und Museum für Geologie und Paläontologie, Tübingen, Germany; **IML**, Instituto Miguel Lillo, Universidad Nacional de Tucumán, San Miguel de Tucumán, Argentina; **MACN**, Museo Argentino de Ciencias Naturales, Buenos Aires, Argentina; **MCNSJ**, Museo de Ciencias Naturales, Universidad Nacional de San Juan, San Juan, Argentina; **NHMUK**, Natural History Museum, London, U.K.; **SAM**, Iziko South African Museum, Cape Town, South Africa; **UFRGS-PV**, Instituto de Geociências, Universidade Federal do Rio Grande do Sul, Porto Alegre, Brazil.

Anatomical Abbreviations—**ac**, anterior condyle; **ace**, atlas centrum; **adc**, adductor crest; **aic**, atlas intercentrum; **ampe**, insertion area of part of M. puboischiofemoralis externus; **ana**, atlas neural arch; **ap**, acromion process; **apaxzns**, anterior process of axis neural spine; **aptz**, atlas postzygapophysis; **apz**, atlas prezygapophysis; **axc**, axis centrum; **axic**, axis intercentrum; **axnc**, axis neural canal; **axns**, axis neural spine; **axtp**, axis transverse process; **axvk**, axis ventral keel; **caf**, facet for calcaneum; **ce**, cervical epipophysis; **cef**, facet for centrale; **cf**, coracoid foramen; **dpc**, deltopectoral crest; **e**, epipophysis; **ect**, ectepicondyle; **ent**, entepicondyle; **entg**, entepicondylar groove; **fana**, facet for atlas neural arch; **ff**, facet for fibula; **gc**, glenoid cavity; **if**, intertrochanteric fossa; **it**, internal trochanter; **lg**, ligament groove; **na**, neural

*Corresponding author.

arch; **nc**, neural channel; **ns**, neural spine; **p**, parapophyses; **pa**, popliteal area; **pb**, posterior boss; **pc**, posterior condyle; **pp**, posterolateral peg; **ppaxns**, posterior process of axis neural spine; **ptz**, postzygapophysis; **pz**, prezygapophysis; **vc**, vertebra centrum; **vk**, ventral keel; **sd**, shaft depression; **sg**, superficial groove; **sgb**, supraglenoid buttress; **sr**, supinator ridge; **tasc**, trochanteric area for the insertion of *M. subcoracoscapularis*; **tc**, tibial crest; **tf**, facet for tibia; **tp**, transverse process.

SYSTEMATIC PALEONTOLOGY

DIAPSIDA Osborn, 1903

RHYNCHOSAURIA (Gervais, 1859) Osborn, 1903

HYPERODAPEDONTINAE Chatterjee, 1969 (nom. trans.
ex Lydekker, 1885)

TEYUMBAITA Montefeltro, Langer, and Schultz, 2010

TEYUMBAITA SULCOGNATHUS (Azevedo and Schultz,
1987)

(Figs. 1–18)

Diagnosis—Rhynchosaur with anterior margin of nasal concave at midline; prefrontal separated from the ascending process of the maxilla; palatal ramus of pterygoid expanded laterally within the palatines; markedly depressed dorsal surface of the exoccipital; and a single tooth lingually displaced from the main medial tooth-bearing area of the maxilla.

Appended Postcranial Diagnosis—Glenoid cavity formed mostly by the scapula; groove with elevated borders on the external surface of the entepicondyle; and transverse bar on the posterior surface of the astragalus extending from the lateral astragalar peg to the centrale articular facet (on the opposite side of the bone).

Description and Comparisons—The following description is based on the holotype (UFRGS-PV-0232T) and referred specimens (UFRGS-PV-0298T and PV-0290T) of *Teyumbaita sulcognathus*. The three specimens together have most of the postcranial elements preserved, although the holotype has the greater number of elements, including cervical, trunk, and caudal vertebrae, pectoral girdle, forelimbs, and hind limbs. UFRGS-PV-0298T has the axis and few trunk vertebrae, and UFRGS-PV-0290T has four trunk vertebrae and part of the left hind limb, including the astragalus. The postcranial remains were described following the osteological nomenclature employed by Romer (1966), Langer and Schultz (2000), and Whatley (2005). Previous studies suggested that rhynchosaurs had the forelimb in a partly sprawling position, but the hind limbs in a semierect position (Benton, 1983, 1990). Following this suggestion, the

positional terms used in the forelimb description refer to a horizontally oriented humerus, whereas the hind limb elements are described vertically oriented. The postcranial remains of *T. sulcognathus* were compared within the context of total rhynchosaur diversity, although special attention was given to the morphology of taxa with more complete postcrania. *Otiischalkia elderae* Hunt and Lucas, 1991, was not used for the comparisons given that its rhynchosaurian affinity has been challenged (Long and Murry, 1995; S. Nesbitt and M. Stocker, pers. comm., March 2012). Clades mentioned in the description follow the definitions of Langer et al. (2010).

As previously described for the cranial remains of UFRGS-PV-0232T and PV-0298T (Montefeltro et al., 2010), the preserved postcranial bones are lightly built (Tables 1–4) in comparison with other hyperodapedontines (Huene, 1929, 1942; Sill, 1970; Chatterjee, 1974; Benton, 1983). As an example, the holotype femur has the ratio of the total length/shaft width of 6.9 and the same ratio in UFRGS-PV-0290T is 5.2. In contrast, UFRGS-PV-0290T is larger and more robust than the other specimens of *T. sulcognathus*.

Vertebral Column—The atlas-axis complex is virtually complete in the holotype, the atlantal intercentrum and neural arches are preserved separately (Fig. 1) from the remaining elements (atlantal centrum, axial centrum, and intercentrum), which are articulated with the next four neck vertebrae (Figs. 2, 3). In UFRGS-PV-0298T, only the axial neural arch is preserved but not fully prepared, preventing an accurate description.

The atlantal intercentrum is a dorsally concave and ventrally convex semicylindrical element. This morphology resembles the condition observed in *Stenaulorhynchus stockleyi* Haughton, 1932, and *Hyperodapedon huxleyi* Lydekker, 1885, but differs from the spatulate atlantal intercentrum of *Hyperodapedon gordonii* Huxley, 1859. The depth of the intercentrum dorsal concavity decreases posteriorly, and accounts for the greater robustness of the posterior articular facet. The latter is kidney-shaped in posterior view, and ventrally projected.

The unfused atlantal neural arches are about twice as tall as the intercentrum and are erect structures. Their medial surface is concave with a slight inwards curvature in the dorsal portion. The posterior margins of their convex ventral surfaces are slightly elevated relative to the anterior margins, and articulate with faint concavities on the dorsolateral margins of the intercentrum. As described for *H. huxleyi* (Chatterjee, 1974), the neural arches possess elliptical and obliquely oriented anterior surfaces that are continuous to the semicylindrical cranial facet of the intercentrum. These form the atlantal ring (Romer, 1956) that receives the occipital condyle.

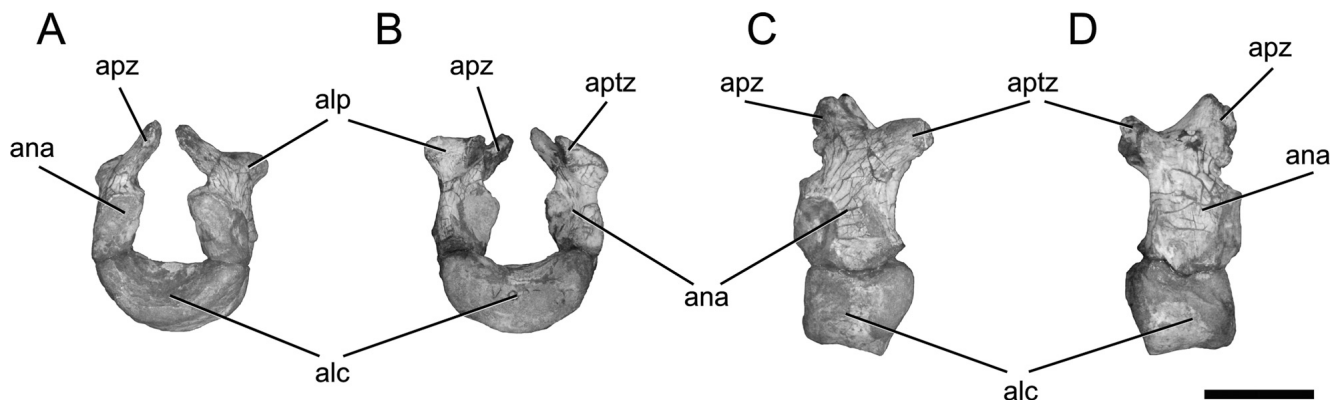


FIGURE 1. *Teyumbaita sulcognathus* (UFRGS-PV-0232T). Atlantal intercentrum and neural arches. **A**, anterior; **B**, posterior; **C**, left; **D**, right lateral views. Scale bar equals 2 cm.

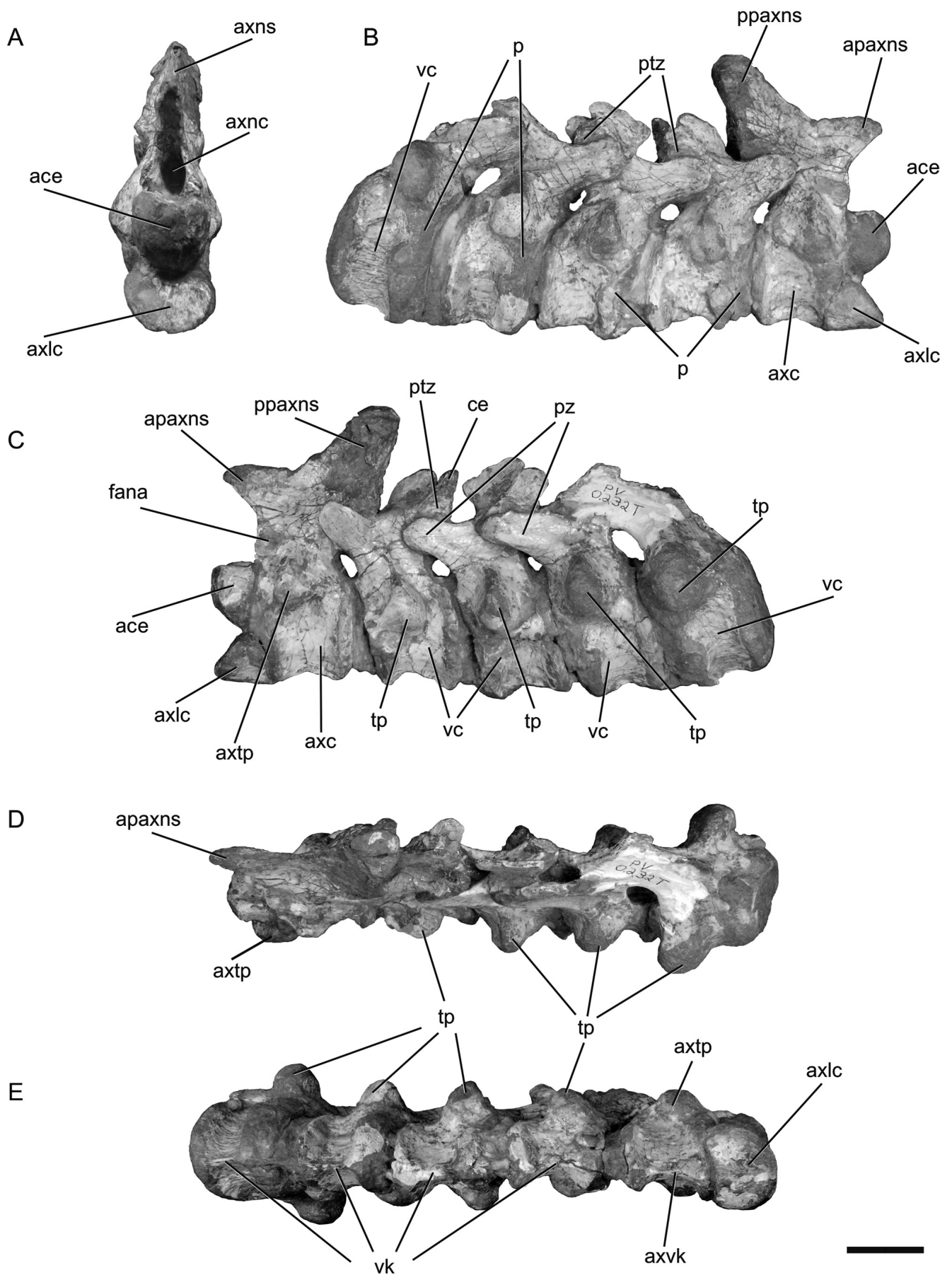


FIGURE 2. *Teyumbaita sulcognathus* (UFRGS-PV-0232T). Axis and following four cervical vertebrae. **A**, anterior; **B**, right lateral; **C**, left lateral; **D**, dorsal; **E**, ventral views. Scale bar equals 2 cm.

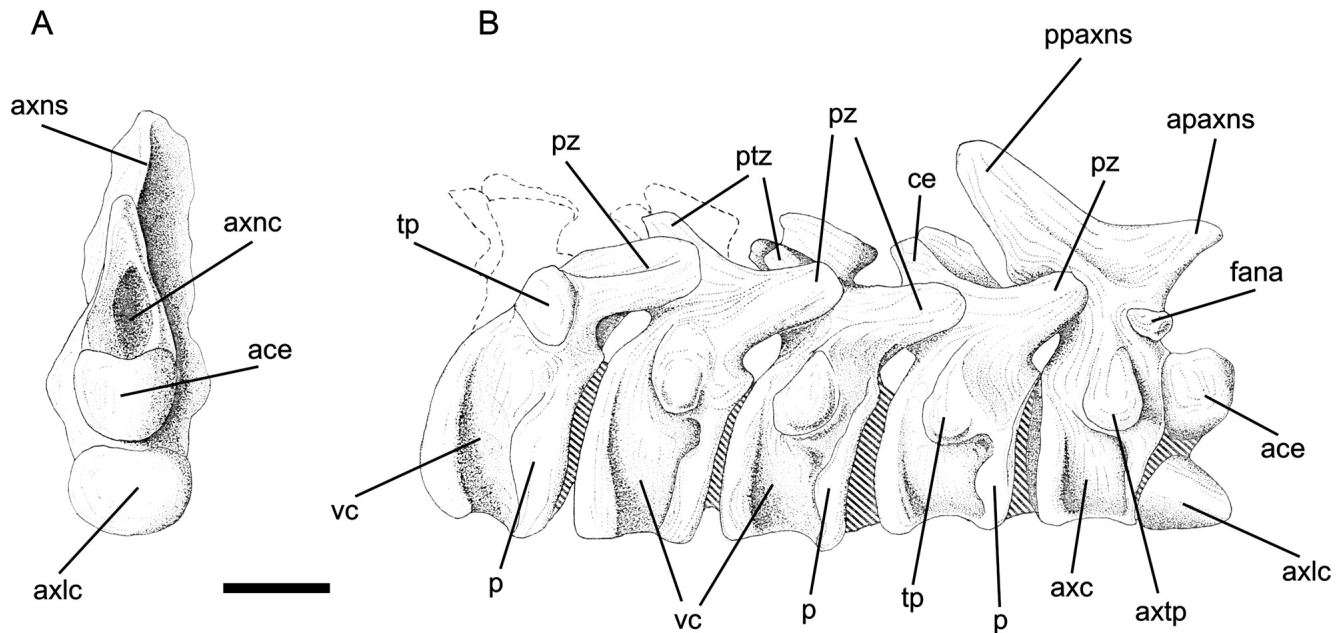


FIGURE 3. *Teyumbaita sulcognathus* (UFRGS-PV-0232T). Schematic drawings of axis and following four cervical vertebrae. **A**, anterior view; **B**, right lateral view. Modified from Schultz (1986). Scale bar equals 2 cm.

The dorsal half of each neural arch is triradiate, including the prezygapophysis anteriorly, the transverse process laterally, and the postzygapophysis posteriorly. The prezygapophysis projects anteromedially towards its counterpart. There is no medial contact, but each almost reaches the ventral portion of the elongated anterior process of the axial neural spine. The postzygapophysis has an anteroposteriorly and mediolaterally tapering proximal tip, and convex medial and lateral surfaces. An excavation immediately dorsal to the articular area forms a rudimentary infrazygapophyseal fossa. The postzygapophysis corresponds to a posterodorsally and medially oriented process, the articular facet of which is straight, dorsoventrally elongated, and medioventrally directed. It articulates with the axial neural arch via a lateral excavation located between the transverse process and the anterior process of neural spine. The rod-like transverse process is posterolaterally and dorsally oriented. It is subtriangular in dorsal view, and its posterior margin does not reach the posterior-most limit of the postzygapophysis, from which the transverse process is separated by a short concave surface.

The posterior articular facet of the atlantal intercentrum has a beveled contact with the anterior surface of the axial intercentrum, and the space surrounded by the atlantal neural arches is occupied by the anteriorly projecting atlantal centrum. Because the articulation between the atlantal and axial intercentra is inclined, the dorsal margin of the former lies significantly above the latter. The atlantal centrum (odontoid process) is a very prominent anteriorly directed process, attached to the anteroventral portion of the axial centrum and neural arch. In lateral view, its ventral and dorsal margins are straight but not parallel to one another and the distal margin is convex. Unlike the condition in *H. huxleyi* (Chatterjee, 1974), no specimen attributed to *T. sulcognathus* shows evidence of a proatlas.

The axial intercentrum is subtriangular in lateral view, ventrally flat, and with an oblique anterior margin for contact with the posterior facet of the atlantal intercentrum. Anteriorly, the axial intercentrum is semicircular with a dorsal concavity, similar to the condition described for *S. stockleyi* and *H. huxleyi* (Huene, 1938; Chatterjee, 1974). By contrast to *H. gordonii*

(Benton, 1983), the axial intercentrum of *T. sulcognathus* is not reduced, and is half the height of the axial centrum.

The axial centrum possesses an oval cross-section, with concave lateral walls, and thick anterior and posterior margins. The articular facets are vertically oriented, so that the centrum is subquadrangular in lateral view. As in postaxial cervical vertebrae, the ventral margin of the axis bears a conspicuous keel along its entire length, a feature also observed in *Mesosuchus browni* Watson, 1912, and *Howesia browni* Broom, 1906 (Dilkes, 1995, 1998). The three small bulbous processes present on the anteroventral surface of the axis of *H. gordonii* (Benton, 1983) are not present in *T. sulcognathus* or in other hyperodapedontines (Chatterjee, 1974; IGMPT-23, IML-3432, MCNSJ-680). The axial parapophyses apparently correspond to small rugose facets on the anterior midheight of the lateral surfaces of the centrum. They are dorsally bound by the neural spine and anteroventrally by the contact area between the atlantal centrum and axial intercentrum.

The morphology of the axial neural spine of *T. sulcognathus* is variable. In the holotype, it bears anterior and dorsal processes, as seen in *Rhynchosaurus articeps* Owen, 1842 (Benton, 1990), whereas in UFRGS-PV-0298T it is fan-shaped, as in *M. browni* (Dilkes, 1998), *S. stockleyi* (Huene, 1938), *H. gordonii* (Benton, 1983), *H. huxleyi* (Chatterjee, 1974), and the South American *Hyperodapedon* (IGMPT-23, IML-3432, MCNSJ-680). That trait in the holotype was used to diagnose the taxon by Azevedo and Schultz (1987), but regarded by Schultz (1991) as a taphonomic artifact. We consider this an inherent feature, and suggest that the region between both processes was capped by cartilage, as proposed for *R. articeps* and *H. gordonii* (Benton, 1983, 1990). This variation may result from different ontogenetic stages, sexual dimorphism, or intraspecific variation.

The axial neural arch is twice as tall as the centrum, and the distance between the ventral margin of the transverse process and the base of the anterior process of neural spine accounts for half of its height. The short pyramidal transverse process projects lateroventrally, marking the anteroventral edge of the neural arch. From the dorsal margin of the transverse process, a

lamina projects posterodorsally, reaching the level of the prezygapophysis of the following vertebra.

The anterior process of the neural spine emerges from the anterodorsal margin of the neural arch as a triangular structure. Its dorsal margin is roughly horizontal, but the ventral margin forms an angle of about 40° with the longitudinal plane of the cervical column. The anterior margin of the process does not project further than the anterior margin of the axial intercentrum. The posterior process of the neural spine constitutes about one-third of the neural arch height and its base is much longer than its apex. It projects posterodorsally, with the anterior margin forming an angle of about 140° with the dorsal margin of the anterior process. The posterior margin of the posterior process is more vertical, and bears a dorsoventral sulcus for interspinous ligaments.

Anteroventral to the base of the neural spine, on the lateral margin of the pedicels surrounding the neural canal, a rugose, elliptical, and anteroposteriorly oriented surface corresponds to the articular facet for the atlantal postzygapophysis. The axial postzygapophysis is dorsoventrally deep, medioventrally directed, and linked to the posterolateral margin of the neural spine by a thin lamina.

The presence of a distinct structure on the anterolateral surface of the axial centrum of *T. sulcognathus*, probably homologous to the parapophysis of the following cervical vertebrae, suggests the occurrence of an axial rib. This is also the case for *S. stockleyi* (Huene, 1938), the Brazilian *Hyperodapedon* (IGMPT-19.2; Huene, 1942), and *M. browni* Dilkes (1998), but not for *H. gordonii* (Benton, 1983), which seems to lack this rib.

The following four articulated vertebrae and an additional isolated cervical vertebra have similar morphology. Based on the position of the transverse process and the size and shape of the isolated vertebra, it probably represents the seventh cervical. The number of cervical vertebrae is variable in Rhynchosauria. *Stenaulorhynchus stockleyi* possesses seven cervicals and one transitional vertebra (Huene, 1938); *M. browni* (Dilkes, 1998), *R. articeps* (Benton, 1990), *Isalorhynchus genovefae* Buffetant, 1983 (Whatley, 2005), *H. gordonii* (Benton, 1983), and *H. huxleyi* (Chatterjee, 1974) possess eight cervical vertebrae. By contrast, Huene (1942) suggests the presence of six cervicals and one transitional vertebra in the Brazilian *Hyperodapedon*. The postaxial cervical vertebrae have subelliptical amphicoelous centra. The lateral walls are excavated, markedly on the medioventral portion, forming a well-developed ventral keel, as in *Hyperodapedon* (IGMPT-19.2 and -23; Huene, 1942; Chatterjee, 1974; Benton, 1983) and *Isalorhynchus* (Whatley, 2005). As in all rhynchosaurians, no intercentrum is present in the cervical series.

The transverse processes of cervical vertebrae 3–5 are subtriangular in lateral and dorsal aspects. Moving posteriorly along the preserved cervical series, the processes gradually occupy a more dorsal position on the neural arch. The transverse process of the sixth vertebra is distally rounded and stouter than those of the preceding vertebrae. As in *Hyperodapedon* (Huene, 1942; Chatterjee, 1974), the parapophyseal facets are not clear in *T. sulcognathus*. Yet, the position of that structure can be inferred from the laterally thickened anterior margin of the centrum, anteroventral to the transverse process. In *T. sulcognathus*, these articular surfaces are dorsoventrally expanded, but their shape varies from subtriangular in the third cervical, to rounded in the sixth cervical.

The neural arches are partially preserved in the first four postaxial cervical vertebrae. In dorsal view, the prezygapophyses diverge to form an angle of 30° with each other, and the articular facets are nearly vertical. They cover the well-developed postzygapophyses of the preceding vertebra laterally, except in the third cervical in which the prezygapophyses cover laterally the extremely reduced axial postzygapophyses at the base of the posterior process of the axis neural arch. The postzygapophyses have a subtriangular shape in lateral view, and their articu-

lar facets face laterally, also diverging at an angle of 30° in dorsal view.

The postzygapophyses of the third cervical vertebra possess a well-developed epipophysis on the left side. This structure is crest-shaped, dorsally tapering, and also observed in transverse sections of the postzygapophyses of the fourth and probable ninth presacral vertebrae (for discussion on rhynchosaurian cervical epipophyses, see Whatley, 2005).

Another isolated vertebra of the holotype (Fig. 4F–J) is the best-preserved trunk element of *T. sulcognathus*. Due to the position of the transverse process and the robustness of the centrum, it probably represents the eighth or ninth vertebra. It shares traits with the articulated and isolated more anterior cervical vertebrae and can be regarded as a ‘transitional’ element, as described for *S. stockleyi* and the Brazilian *Hyperodapedon* (Huene, 1938, 1942).

The amphicoelous centrum is rounded in cross-section, the lateral walls of which are slightly excavated. It lacks the typical ventral keel of the cervical vertebrae. On its dorsolateral portion, the neural arch transverse process expands as in the inferred seventh cervical vertebra. As in the cervical vertebrae, the parapophyseal region lies anteroventral to the transverse process. However, the parapophysis is less prominent and further displaced dorsally, showing the beginning of a trend towards confluence with the transverse process in the more posterior trunk vertebrae.

In dorsal view, the prezygapophyses diverge at an angle of 30°. Their dorsomedially oriented articular facets cover the postzygapophysis of the preceding vertebra ventrolaterally. Each postzygapophysis is subtriangular in lateral view, and forms an angle of 30° with the midline. The articular facet is lateroventrally oriented, with a dorsal epipophysis, as in the cervical vertebrae. This is not fully preserved, but the preserved portion suggests that it is less developed than in the cervical vertebrae.

The neural spine is a blade-like element, and is about one-half of the centrum height. It is located posterior to the centrum midlength, on the posterodorsal region of the neural arch. In lateral view, this process is roughly semicircular in outline, with the posterior edge perpendicular to the main axis of the vertebral column. The anterior edge forms a continuous curve from the base to the dorsal tip. In posterior view, the neural spine possesses a longitudinal groove that is ventrally deeper and wider.

Four more posterior trunk vertebrae are preserved in the holotype. These show two distinct morphologies associated with their positions within the series, as seen in the complete vertebral series of *Hyperodapedon* (e.g., UFRGS-PV-0408T, IGMPT-19.2 and -23; Chatterjee, 1974; Benton, 1983). The preserved centra are all amphicoelous, and circular in cross-section. They have depressed lateral walls, but no ventral keel as those of *H. gordonii* (Benton, 1983). No neural arch is complete, but a sinuous suture marks the boundary with the centrum.

The transverse processes are more expanded laterally than in the preceding vertebrae, being located more posteriorly on the centra. Indeed, the dorsal edges of the transverse processes are located above the level of neural channel roof, following the trend of dorsalization of that structure, already observed in more anterior vertebrae. In anterior view, the dorsal surface of the transverse processes forms a right angle with the neural arch. By contrast, its ventral surface is oblique to the lateral wall of the centra, so the process has a subtriangular anterior outline (Fig. 5A–F). Conversely, in the two posterior-most preserved trunk vertebrae, the ventral surface is also perpendicular to the lateral surface of the centrum (Fig. 5G–L). The neural spines are damaged and no relevant information is available.

Four trunk vertebrae are preserved in UFRGS-PV-0290T (Fig. 6). Two are middle trunk vertebrae (Fig. 6D–I, trunks c and d of Table 1), whereas the remaining two elements (Fig. 6A–C, J–L) are assumed to be more anteriorly (trunk b of Table 1) and posteriorly (trunk e of Table 1) placed, respectively. Basically,

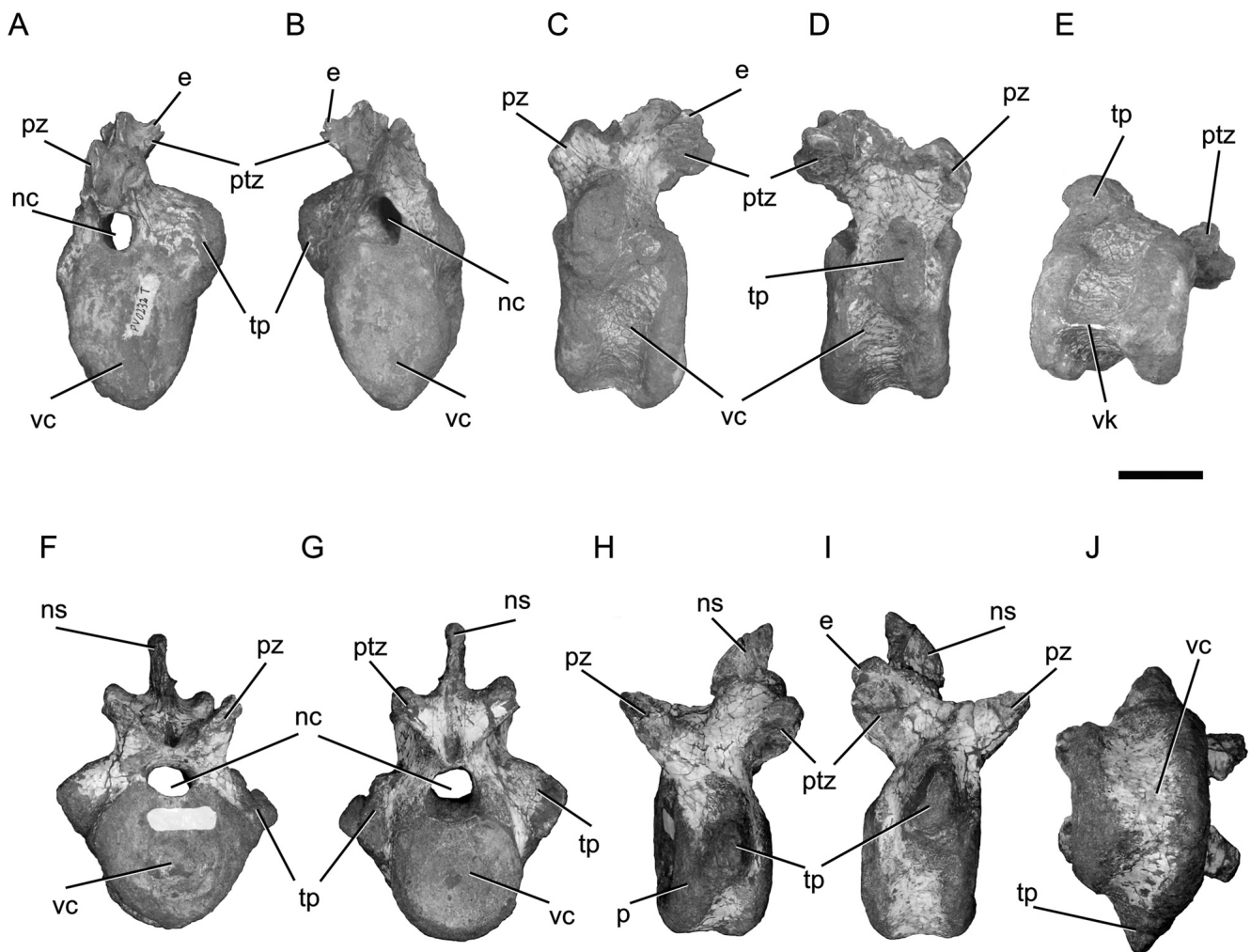


FIGURE 4. *Teyumbaita sulcognathus* (UFRGS-PV-0232T). Isolated cervical (A–E) and trunk (F–J) vertebrae. A and F, anterior views; B and G, posterior views; C and H, left lateral views; D and I, right lateral views; E and J, ventral views. Scale bar equals 2 cm.

these share the same morphology as the holotype vertebrae, but their preservation does not allow a detailed comparison. One remarkable difference is their size (Table 1): the centra are about twice the length of other specimens, which is congruent with the size of the respective cranial material (Montefeltro et al., 2010). In addition, the transverse process of the more posterior trunk vertebra of UFRGS-PV-0290T is dorsoventrally narrower than those of the holotype, resulting in its bar-like shape in anterior view. Some trunk elements are also preserved in UFRGS-PV-0298T, but little information can be recovered due to lack of preparation.

There is a significant discrepancy in the estimation of the number of caudal vertebrae in rhynchosaurs varying from approximately 25 to as many as 50 based on relatively complete specimens (Chatterjee, 1974; Carroll, 1976; Benton, 1990; Dilkes, 1995, 1998). The exact number of caudal vertebrae of *T. sulcognathus* is unknown, but at least 16 elements are partially preserved in the holotype. It is not possible to determine whether the vertebrae form a continuous series. The weakly developed transverse processes suggest a distal position in the tail for all elements (Fig. 7). The centra are rounded in cross-section and are more amphicoelous than the trunk elements. In ventral view, they are as laterally compressed as in *H. gordonii* and *H. huxleyi* (Benton, 1983).

The tail neural arches are only partially preserved, but their general morphology is basically the same as that of the cervical and trunk vertebrae. The preserved transverse processes are located at the midheight of the vertebrae and are subtriangular in anterior and posterior views. Ventrally, the elliptical chevron facets are positioned on the posteroventral margin of the centrum.

Rib fragments are preserved in UFRGS-PV-0298T. Their transverse cross-sections are variably circular to elliptical. Two proximal rib portions are partially preserved, and their di-cephalous morphology suggests that they are from either a cervical or anterior-most dorsal rib. The gastralia are also partially preserved in the holotype. They are fragile rod-like elements, frequently recognized only by their outlines on small blocks of sediment. These are circular to elliptical in cross-section, but the preservation does not allow recognition of the ‘V’-shaped pattern seen in other rhynchosaur gastralia (Benton, 1983, 1990; Dilkes, 1998).

Forelimb—The holotype includes a complete left and a partial right scapulocoracoid in which the dorsal half of the scapula blade is missing (Figs. 8, 9). Remarkable differences are observed between these elements. The left girdle was described together with the corresponding humerus by Schultz (1986), who proposed an unprecedented forelimb position for the taxon. However,

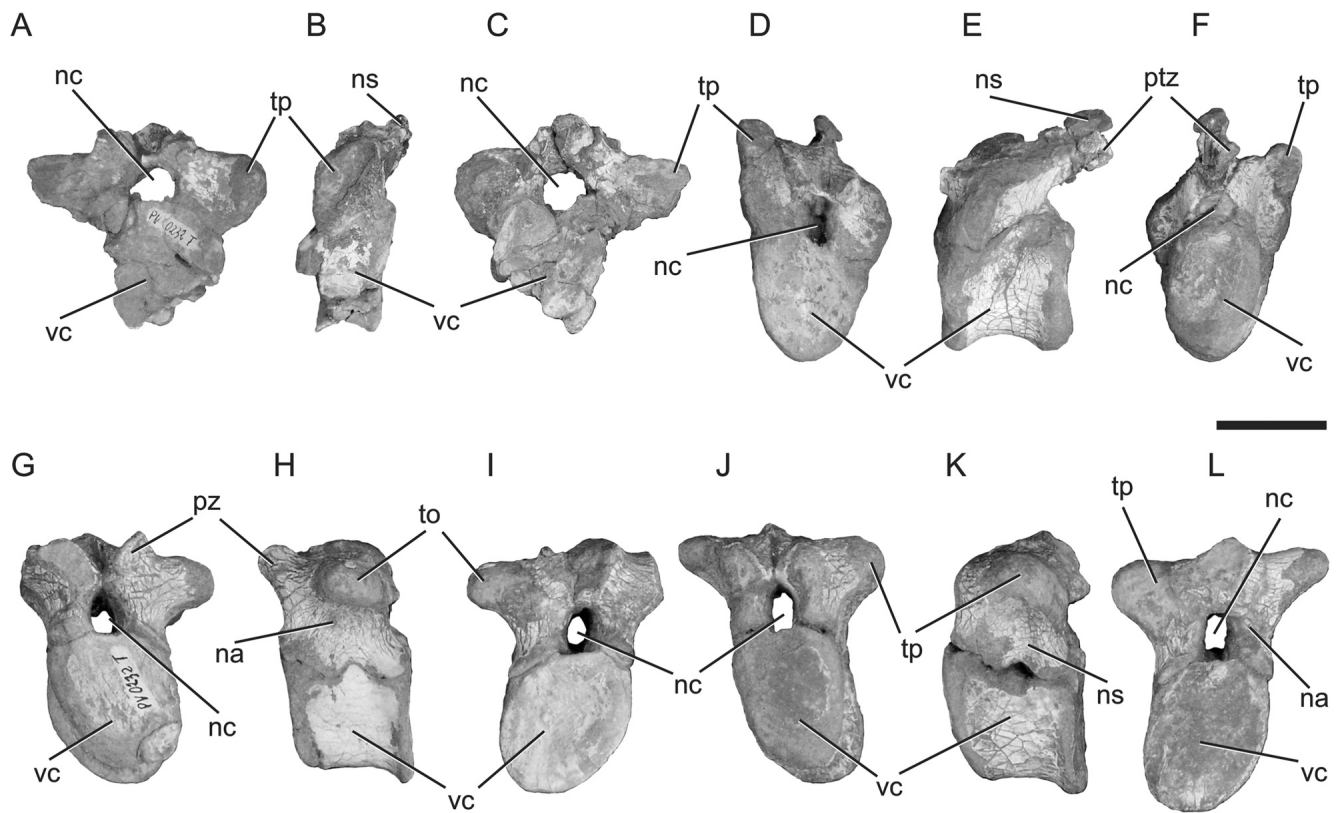


FIGURE 5. *Teyumbaita sulcognathus* (UFRGS-PV-0232T). Anterior (A–F) and posterior (G–L) trunk vertebrae. A, D, G, and J, anterior views; B, E, H, and K, left lateral views; C, F, I, and L, posterior views. Scale bar equals 2 cm.

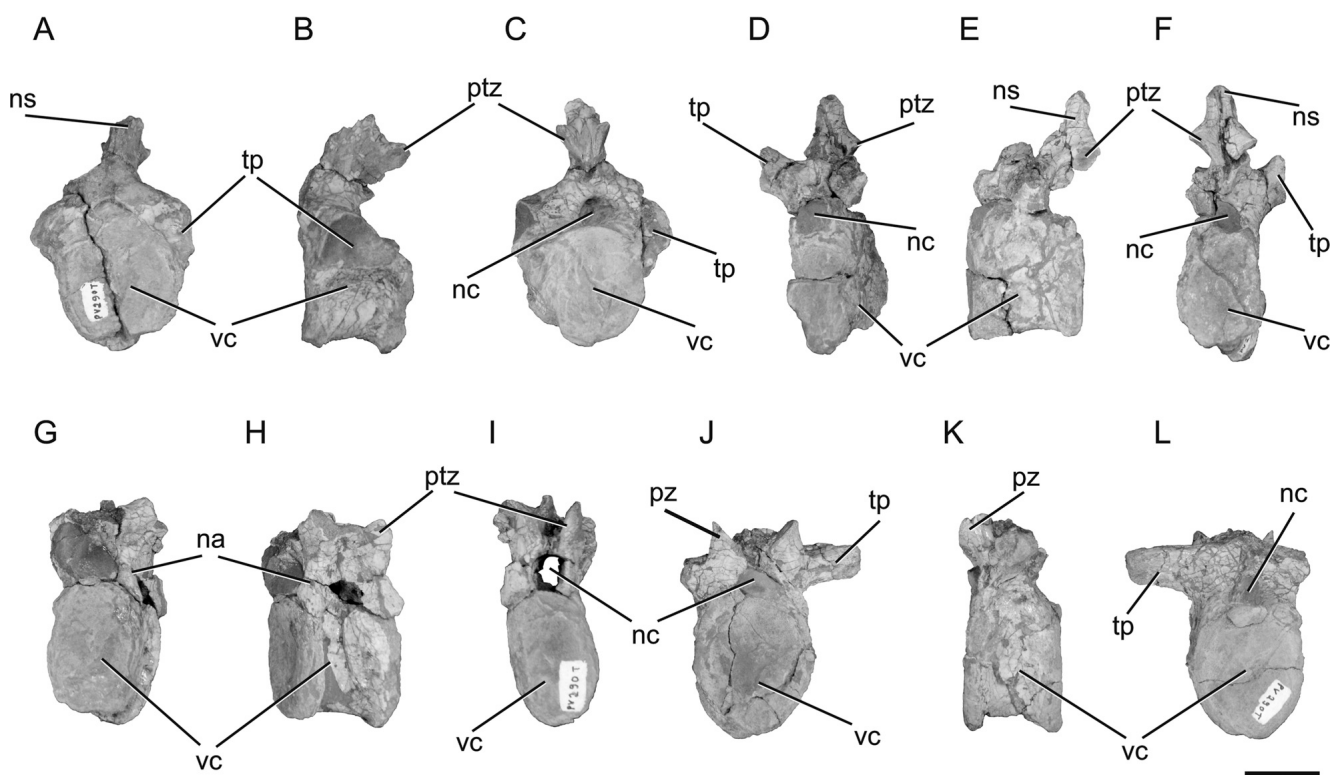


FIGURE 6. *Teyumbaita sulcognathus* (UFRGS-PV-0290T). Anterior (A–C), median (D–I), and posterior (J–L) trunk vertebrae. A, D, G, and J, anterior views; B, E, H, and K, left lateral views; C, F, I, and L, posterior views. Scale bar equals 2 cm.

TABLE 1. Vertebra measurements (in cm) of *Teyumbaita sulcognathus*.

Vertebra	Centrum length	Centrum height	Centrum width
UFRGS-PV-0232T			
Atlas	1.4	1.6	1.9
Axis	2.6	2.9	1.7
	Intercentrum length	Intercentrum height	Intercentrum width
Atlas	2.0	1.6	3.5
Axis	1.8	1.7	2.3
	Centrum length	Centrum height	Centrum width
Cervical 3	2.5	3.1	1.8
Cervical 4	2.3	3.5	1.9
Cervical 5	2.4	3.8	2.3
Cervical 6	2.7	3.8	3.0
Cervical 7	2.9	4.0	2.9
Anterior trunk a	2.6	3.4	4.0
Anterior trunk b	1.5	3.4	2.9
Anterior trunk c	3.2	3.4	2.4
Posterior trunk a	2.6	2.8	2.2
Posterior trunk b	2.2	2.8	2.3
Caudal a	2.5	2.4	2.1
Caudal b	2.2	2.6	2.3
Caudal c	2.2	2.1	1.5
Caudal d	2.1	2.5	1.8
Caudal e	2.1	1.6	1.5
Caudal f	2.1	2.1	1.5
Caudal g	2.1	1.6	1.4
Caudal h	2.0	1.1	1.0
Caudal i	1.8	1.4	1.1
Caudal j	1.8	1.2	1.1
Caudal k	1.8	1.1	0.9
Caudal l	1.7	1.0	1.1
Caudal m	1.5	1.3	0.9
Caudal n	1.4	0.9	0.9
Caudal o	1.3	1.5	1.3
Caudal p	1.1	0.8	0.8
UFRGS-PV-0290			
Dorsal a	2.8	3.3	3.6
Dorsal b	4.4	4.1	2.8
Dorsal c	3.9	4.5	3.1
Dorsal d	3.4	4.7	3.9

Caudal vertebrae a-p ordered by centrum length.

more detailed preparation revealed that the unique traits of the appendicular skeleton of UFRGS-PV-0298T result from taphonomic distortion (Schultz, 1991). As a consequence, the right scapulocoracoid is considered more reliable for reconstructing the original positions of the various structures. The differences between these elements are stressed in the following description.

Although similar in profile, the scapulocoracoid of *T. sulcognathus* is more slender than those of *Hyperodapedon* (Huene, 1942; Chatterjee, 1974; Benton, 1983) and *I. genovefae* (What-

TABLE 2. Scapulocoracoid measurements (in cm) of *Teyumbaita sulcognathus*, UFRGS-PV-0232T.

Dimension	Left	Right
Total height	19.3	—
Scapula height	14.1	—
Scapula dorsal length	5.8	—
Scapula ventral length (just dorsal to glenoid)	5.2	4.8
Coracoid height	5.2	6.3
Coracoid length (at ventral portion of glenoid)	6.7	7.5

—, not measurable.

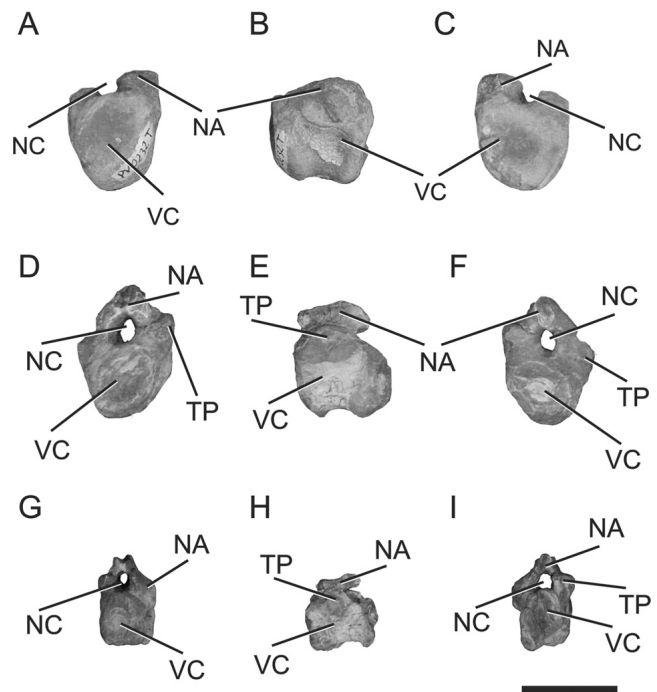


FIGURE 7. *Teyumbaita sulcognathus* (UFRGS-PV-0232T). Three best-preserved caudal vertebrae. **A**, **D**, and **G**, anterior views; **B**, **E**, and **H**, left lateral views; **C**, **F**, and **I**, posterior views. Scale bar equals 2 cm.

ley, 2005). Based on the left element, the scapula is twice the dorsoventral height of the coracoids (see Table 2). On the medial surface, the scapulocoracoid has a shallow dorsoventrally extending groove, spanning from the ventral one-third of the scapula blade to the dorsal margin of the coracoid foramen. The scapula blade has a gently convex dorsal margin, a sigmoid anterior margin, and a nearly straight posterior margin. The coracoid is semicircular in outline, and lacks the posterior process. The latter condition has been regarded as a hyperodapedontine synapomorphy (Benton, 1984, 1985, 1987, 1990; Dilkes, 1995; Langer and Schultz, 2000; Hone and Benton, 2008; Langer et al., 2010; Montefeltro et al., 2010), shared by *I. genovefae* (Whatley, 2005), *H. gordonii* (Benton, 1983), *H. huxleyi* (Chatterjee, 1974), and *Hyperodapedon sanjuanensis* Sill, 1970 (MACN-18185). On the contrary, *M. browni*, *R. articeps*, and *S. stockleyi* possess a well-developed posterior process. In anterior view, both scapula and coracoid are medially concave, following the lateral contour of the ribcage. This curvature is more pronounced in the left scapulocoracoid, but this is a taphonomic distortion. The alleged capping of the entire scapulocoracoid by cartilaginous tissue (Benton, 1983, 1990) cannot be confirmed, but the texture of the dorsal margin of the scapula blade and the ventral margin of the coracoid suggest that these regions were covered by cartilage.

A blunt acromion process is present on the ventral one-third of the scapula anterior margin, dorsal to the level of the glenoid cavity. The acromion is stouter in the left scapula, and occupies a more lateral position, probably due to taphonomic distortions. The right acromion possesses an anterolateral position similar to that of other hyperodapedontines (Chatterjee, 1974; Benton, 1983; UFRGS-PV-0298T, MCNSJ-679, IMGPT-19.2).

The glenoid is deeply excavated at the posterior margin of the scapula-coracoid junction, and is bounded dorsally and ventrally by stout supra- and subglenoid buttresses. On the left side, the glenoid is posteriorly oriented, its borders are robust, and the scapula and coracoid portions form an angle of 90° to one

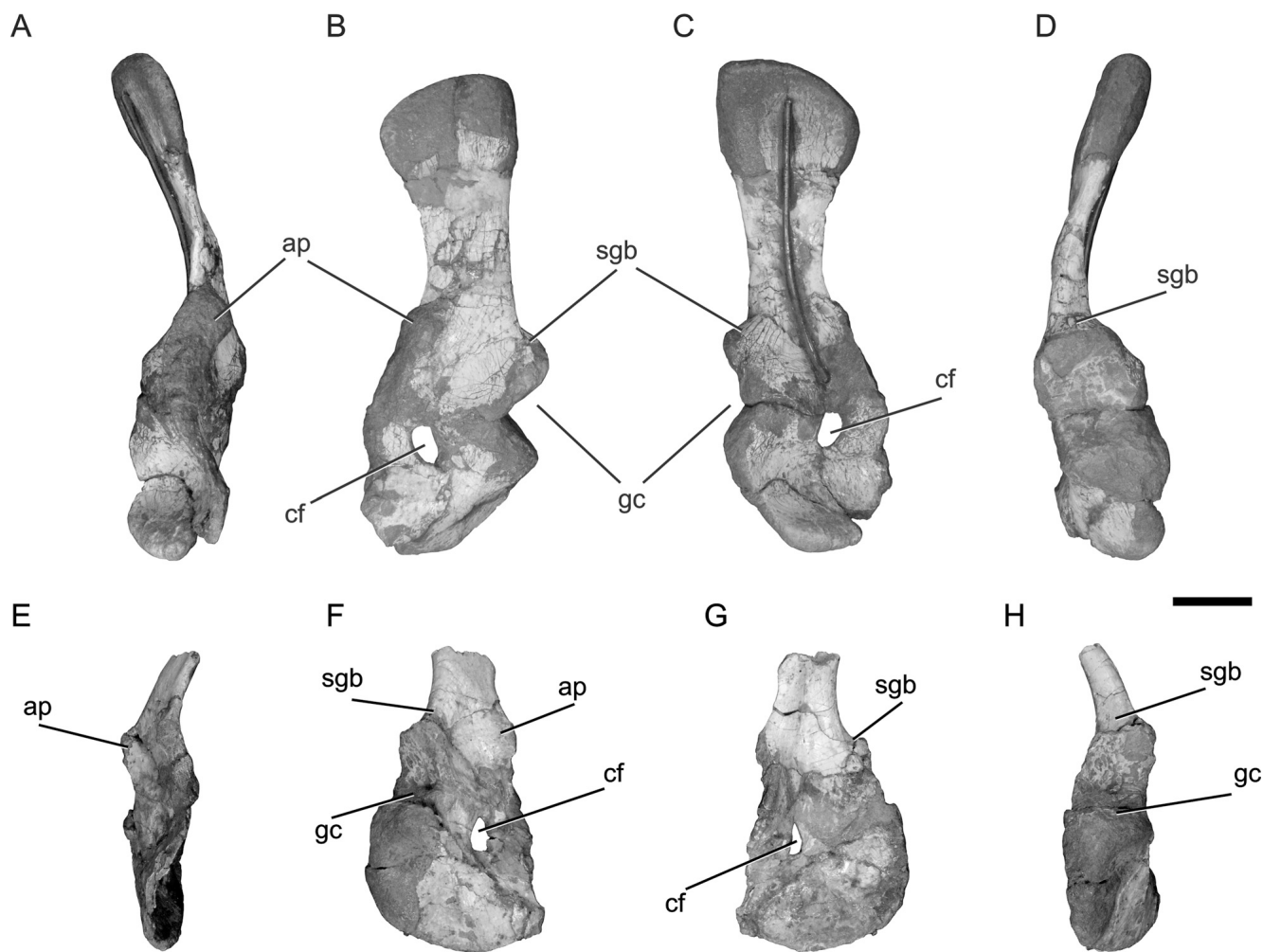


FIGURE 8. *Teyumbaita sulcognathus* (UFRGS-PV-0232T). Left (A–D) and right (E–H) scapulocoracoids. A and E, anterior views; B and F, lateral views; C and G, medial views; D and H, posterior views. Scale bar equals 3 cm.

another. On the right side, the cavity is lateroventrally directed, with smooth borders, and the articular facets diverging at an angle of 105°. As mentioned above, the right side seems to be less affected by taphonomic distortion. In both scapulae, the suture between the scapula and coracoid forms a straight line. It extends onto the glenoid cavity asymmetrically, with greater participation of the scapula. This condition differs from those seen in *M. browni* (Dilkes, 1998), *Rhynchosaurus articeps* (Benton, 1990), *S. stockleyi* (Huene, 1938), *I. genovefae* (Whatley, 2005), *H. gordonii* (Benton, 1983), and *H. huxleyi* (Chatterjee, 1974), and represents an autapomorphic trait of *T. sulcognathus*.

The blade-like coracoid is thicker posteriorly than anteriorly. An elongated foramen pierces its dorsal portion, but enters dorsally into the scapula on the left side. The position of this

structure is highly variable among rhynchosaurs and a foramen entirely rimmed by the coracoid (as in the right side of *T. sulcognathus*) is seen in *R. articeps* (Benton, 1990), *S. stockleyi* (Huene, 1938), and *H.* (Chatterjee, 1974).

The left humerus of the holotype is nearly complete. In UFRGS-PV-0298T, the left humerus lacks the proximal region, and the right one has only its distal portion (Figs. 10, 11). The humerus/femur length ratio (see Tables 3 and 4) is almost 0.7, a plesiomorphic condition also observed in *M. browni* (Dilkes, 1998), *R. articeps* (Benton, 1990), *S. stockleyi* (Huene, 1938), *I. genovefae* (Whatley, 2005), and South American specimens of

TABLE 3. Humerus measurements (in cm) of *Teyumbaita sulcognathus*.

Specimen	Total length	Proximal width	Distal width	Medium shaft width
UFRGS-PV-0232T	13.9	7.6	5.2	1.9
UFRGS-PV-0298T	14.8	8.5	—	2.8

—, not measurable.

TABLE 4. Hind limb measurements (in cm) of *Teyumbaita sulcognathus*.

Femur/Tibia	Total length	Proximal width	Distal width
UFRGS-PV-0232T			
Right femur	19.3	5.1	6.3
Right tibia	14.2	5.8	4.0
UFRGS-PV-0290T			
Right femur	21.6*	—	6.6
Right tibia	20.3	8.6	—

—, not measurable; *, not fully measurable.

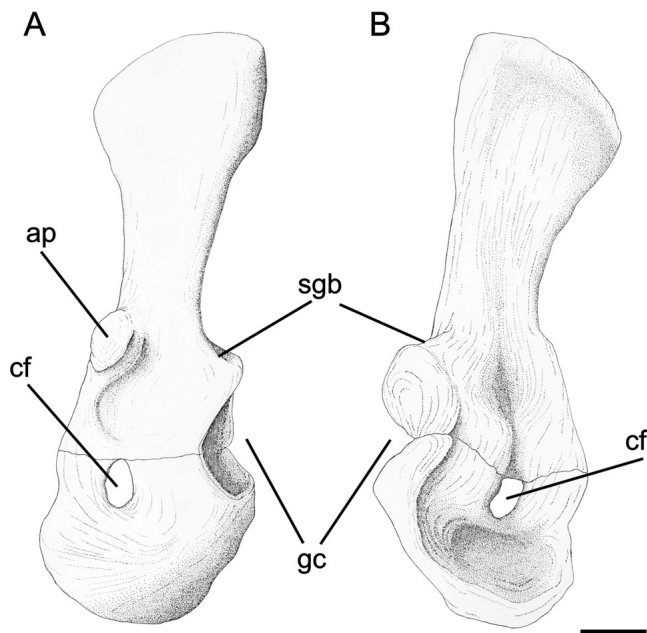


FIGURE 9. *Teyumbaita sulcognathus* (UFRGS-PV-0232T). Schematic drawings of left scapulocoracoid. **A**, lateral view; **B**, medial view. Modified from Schultz (1986). Scale bar equals 2 cm.

Hyperodapedon (UFRGS-PV-0408T, IGMPT-23, MCNSJ-679, MCNSJ-680). In contrast, a ratio of about 1.0 is observed in *H. gordonii* and *H. huxleyi* (Benton, 1983, 1990; Dilkes, 1998; Langer and Schultz, 2000; Hone and Benton, 2008).

The humerus of *T. sulcognathus* is more strongly expanded proximally than distally, with the shaft narrow and nearly cylindrical. In proximal or distal view of the holotypic bone, the long axis of the proximal margin (across the deltopectoral crest and the humeral head) is almost perpendicular to that across the distal condyles, a unique condition among rhynchosaurs. However, the left humerus of UFRGS-PV-0298T (Fig. 12) is more similar to that of other hyperodapedontines, and the holotype condition is probably a taphonomic artifact.

In proximal view, the humeral head of the holotype is anteriorly concave due to the anterior inflexion of the deltopectoral crest, forming an almost continuous curve. The shape of the deltopectoral crest is highly variable among rhynchosaurs. That of *T. sulcognathus* approaches the condition seen in *R. articeps* (Benton, 1990), *I. genovefae* (Whatley, 2005), and *H. gordonii* (Benton, 1983). Conversely, *S. stockleyi* (Huene, 1938), *H. huxleyi* (Chatterjee, 1974), and some South American *Hyperodapedon* specimens (FZB-PV-3509, FZB-PV-3598, MCP-570, UFRGS-PV-0408T) possess a deltopectoral crest that extends almost perpendicular to the humeral head. The articulation with the glenoid is damaged, but the trochanteric area for the insertion of the *M. subcoracoscapularis* is more strongly developed than that of any other known rhynchosaur, with a depressed area on the shaft where the insertion of the muscle and the deltopectoral crest merge together.

The anterodistal portion of the humerus bears a deep and roughly triangular excavation, between the epicondyles. This is probably homologous to the fossa brachialis of birds, basal dinosaurs, and archosaurs in general (Romer, 1956; Baumel and Witmer, 1993; Yates, 2004), being related to the insertion of the *M. brachialis inferior*. The entepicondylar area is less expanded than the rounded ectepicondylar area in the holotype,

but in UFRGS-PV-0298T such expansions are less discrepant in size.

Although badly preserved, the capitellum can be partially recognized as a rugose area on the laterodistal portion of the fossa brachialis, as in *H. gordonii* (Benton, 1983). On the external surface of the ectepicondyle, the supinator process forms a thin crest and a relatively well developed ligament groove, as also seen in *H. sanjuanensis* (MACN-18185), *H. gordonii* (Benton, 1983), and *H. huxleyi* (Chatterjee, 1974), and differing from the hook-shaped supinator process of *S. stockleyi* (Huene, 1938; Hunt and Lucas, 1991). Unique among rhynchosaurs, the entepicondyle of *T. sulcognathus* bears a well-developed lateral groove, flanked by elevated borders, that extends proximally to the proximal portion of the fossa brachialis.

Hind Limb—The right femora of both the holotype and UFRGS-PV-0290T are preserved (Figs. 13, 14, 15). The femur of UFRGS-PV-0290T is larger, and the femur/tibia length ratio is significantly smaller than in the holotype (1.35 for the holotype and 1.06 for UFRGS-PV-0290T). The femur of *T. sulcognathus* possesses the usual rhynchosaurid traits, including the constricted cylindrical shaft and the slight sigmoidal curvature. The articulation areas are expanded, and the ratio between the width across the distal condyles and the length of the bone is greater than 0.3 (see Table 4), giving the femur a stout shape.

The proximal surface of the holotype femur is heavily worn and was probably covered by cartilaginous tissue in life. The well-developed internal trochanter corresponds to a proximodistally oriented crest that is stouter in the holotype than in UFRGS-PV-0290T. This structure is not continuous with the articular area, as also seen in *H. huxleyi* (Chatterjee, 1974), *I. genovefae* (Whatley, 2005), and some South American *Hyperodapedon* specimens (UFRGS-PV-0408T, IGMPT-23, MCNSJ-574, MCNSJ-680, MCNSJ-679). This condition contrasts with that of *M. brownii* (Dilkes, 1998), *H. brownii* (Dilkes, 1995), *S. stockleyi* (Huene, 1938), and *H. gordonii* (Benton, 1983) in which the internal trochanter is continuous with the ventral margin of the articular area. It tapers distally in anterior and posterior views, merging smoothly into the shaft in UFRGS-PV-0290T, but forming a sharper angle in the holotype. The internal trochanter forms the anterior margin of the intertrochanteric fossa, which is more anteroposteriorly developed in the holotype, but broader dorsoventrally in the referred specimen. Posteriorly, the fossa is bounded by a faint crest that starts on the posterior surface of the proximal articulation and extends distally to a small tuberosity. This may correspond to the insertion area of part of the *M. puboischiofemorales externus*, as proposed for *S. stockleyi* (Huene, 1938) and *R. articeps* (Benton, 1990).

The ventral surface of the femur has a robust adductor crest extending from the distal portion of the internal trochanter to the posterior portion of popliteal area, where it is much reduced. In UFRGS-PV-0290T, the proximal extension of the adductor crest reaches the boundary between the anterior and ventral surfaces of the femur, whereas in the holotype, the entire crest is visible in ventral view. The fourth trochanter is lacking in *T. sulcognathus*.

The distal femoral condyles of *T. sulcognathus* conceal the shallow, rhomboidal popliteal fossa. Although not fully preserved in any specimen, it can be inferred that the posterior condyle is more developed than the anterior. Additionally, their worn condition suggests a cartilage capping, as inferred for the other long bones. In the holotype, a shallow depression splits the condyles ventrally.

The right tibiae of both the holotype and UFRGS-PV-0290T are preserved except for their articular ends, and are rather different in general morphology (Figs. 13, 16, 17). The tibia of the holotype is slender, with the proximal end greatly expanded, both lateromedially and anteroposteriorly. In contrast, that of UFRGS-PV-0290T is more robust, and the proximal articular

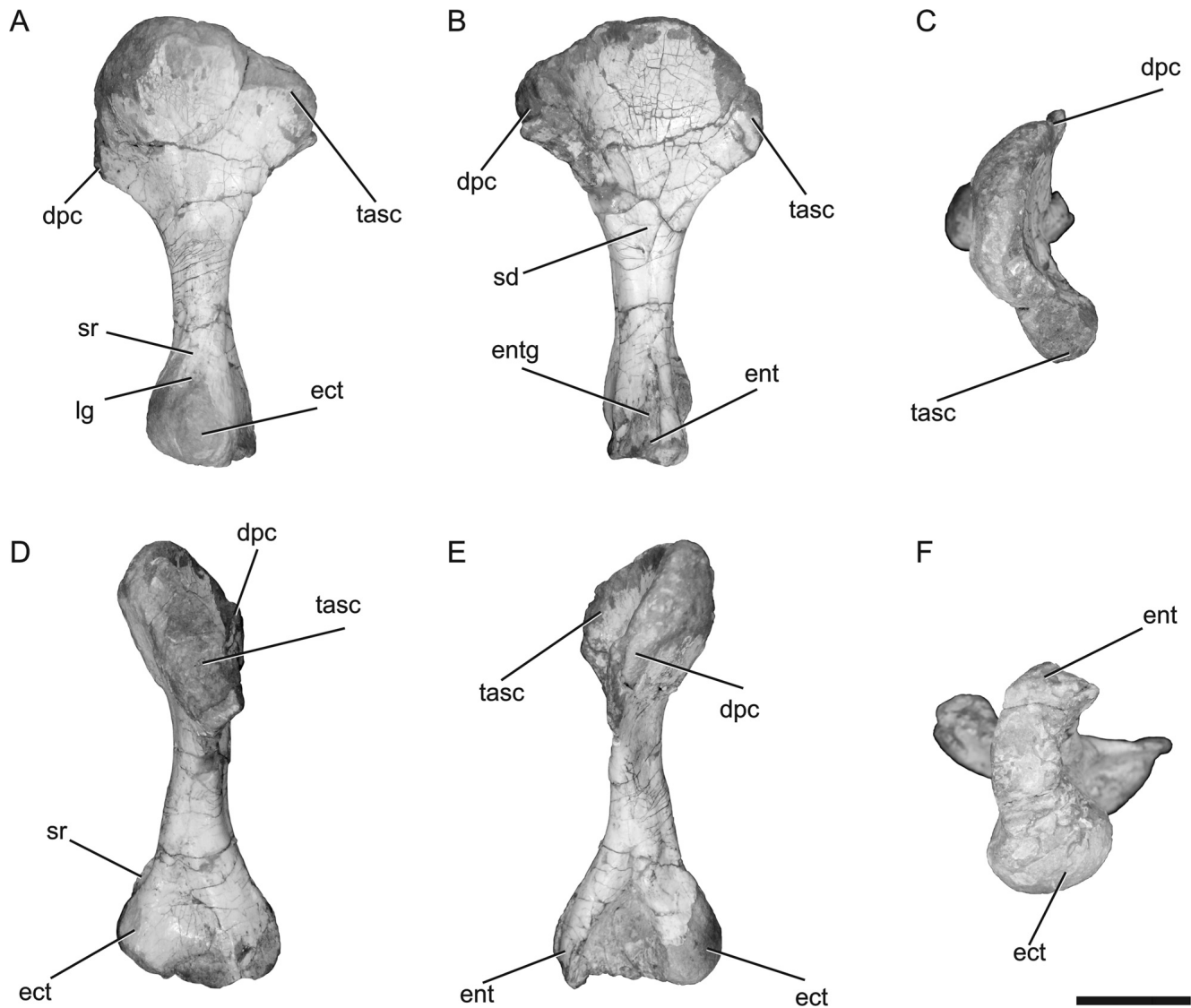


FIGURE 10. *Teyumbaita sulcognathus* (UFRGS-PV-0232T). Left humerus. **A**, anterior view; **B**, posterior view; **C**, proximal view; **D**, dorsal view; **E**, ventral view; **F**, distal view. Scale bar equals 3 cm.

portion less anteroposteriorly expanded. In the holotype, the proximal surface presents an anteroposteriorly directed groove, possibly representing the division of the tibial head for the reception of the femoral condyles, as suggested for *H. gordonii* (Benton, 1983) and *I. genovefae* (Whatley, 2005).

The tibial shaft is ovoid in cross-section and bowed medially away from the fibula, a condition more prominent in UFRGS-PV-0290T. Distal to the proximal head of both specimens, an evident tibial crest extends from the anterolateral to the anteromedial surfaces of the shaft, disappearing before reaching the distal articular end. This crest is absent in *M. brownii* and *H. brownii* (Dilkes, 1995, 1998), but present in *R. articeps* (Benton, 1983), *S. stockleyi* (Huene, 1938), *H. gordonii* (Hone and Benton, 2008), *H. huxleyi* (Chatterjee, 1974), and *I. genovefae* (Whatley, 2005). In addition, the crest is more prominent at its midlength, where a rounded depression related to the extensor musculature is seen. The elliptical distal end of the tibia is badly preserved in both specimens.

Only the proximal portion of the right fibula of UFRGS-PV-0290T is preserved. It is slender in comparison with the tibia, but is more robust than the fibula of *R. articeps* (Benton, 1990) and *S. stockleyi* (Huene, 1938), and more similar to that of *I. genovefae* (Whatley, 2005), *H. gordonii* (Benton, 1983), and *H. huxleyi* (Chatterjee, 1974). Its proximal margin is slightly expanded, and the articular facet is ovoid. On the proximal two-thirds of the incompletely preserved element (probably the proximal half of the bone), the fibula is laterally bowed, forming a large interosseous space with the tibia. In that portion, the shaft is twisted, as clearly indicated by a lateral crest that extends along the midlength of the preserved portion. The medial surface bears a less prominent crest, which starts opposite the lateral crest.

Only the right astragalus of UFRGS-PV-0290T is preserved. It has the typical features of Late Triassic rhynchosaurs, with four clear articular facets: a dorsomedial facet for the tibia, a dorsolateral facet for the fibula, a ventromedial facet for the

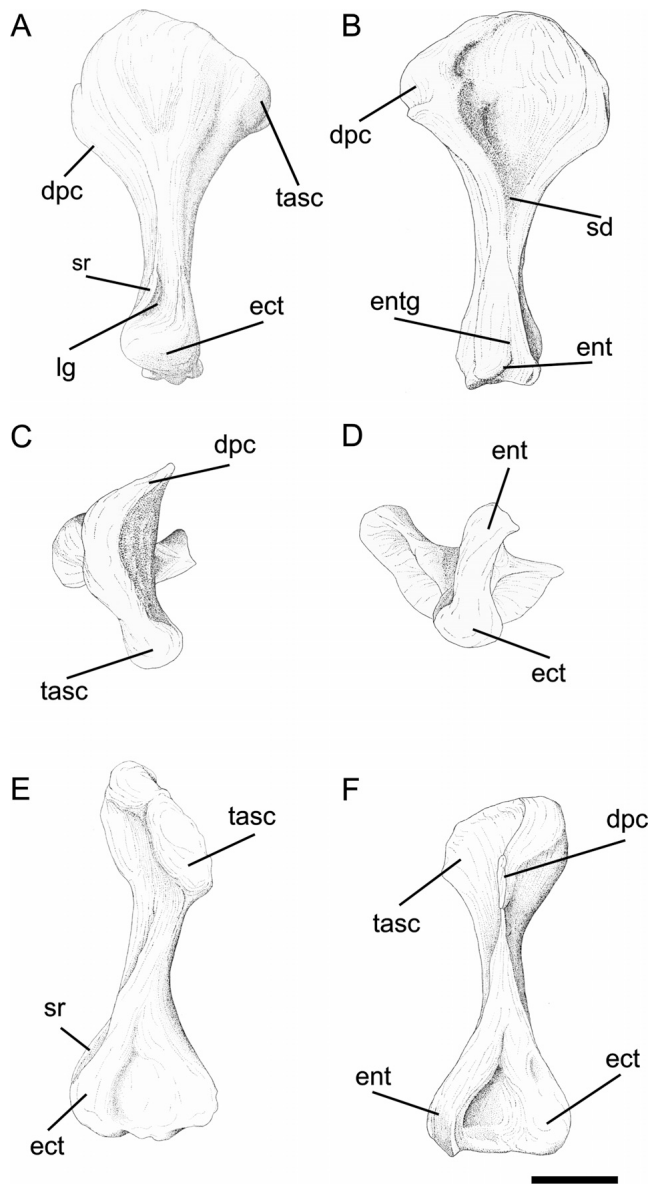


FIGURE 11. *Teyumbaita sulcognathus* (UFRGS-PV-0232T). Schematic drawings of left humerus. **A**, anterior view; **B**, posterior view; **C**, proximal view; **D**, dorsal view; **E**, ventral view; **F**, distal view. Modified from Schultz (1986). Scale bar equals 3 cm.

centrale, and a ventrolateral facet for the calcaneum (Fig. 18). The element is not as robust as those of similar-sized South American *Hyperodapedon* specimens (e.g., UFRGS-PV-0247T, UFRGS-PV-0408T, MCNSJ-574).

Based on the articular facets of the astragalus, the proximal tarsals can be reconstructed as a row of three elements, with the centrale probably of equivalent size to the astragalus, as in other rhynchosaurids (Benton, 1984, 1985, 1987; Dilkes, 1995, 1998; Hone and Benton, 2008). Additionally, the astragalar facet for the centrale is the largest on the bone, as in other hyperodapedontines (Langer and Schultz, 2000; Langer et al., 2000a; Hone and Benton, 2008). The articular facets for the tibia and fibula are smaller and separated by a thin ridge, as described for

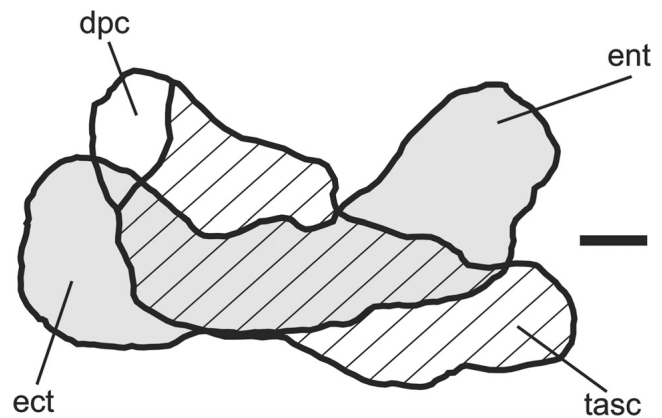


FIGURE 12. *Teyumbaita sulcognathus* (UFRGS-PV-0298T). Schematic outline of the left humerus with articulations superimposed. Proximal articulation dashed and distal articulation in gray. Scale bar equals 1 cm.

H. huxleyi (Chatterjee, 1974). The articular facet for the calcaneum faces lateroventrally; but in contrast to *I. genovefae* (Langer et al., 2000b) and *Hyperodapedon* (UFRGS-PV-0247T), this is not 'U'-shaped. It possesses an excavation bordering the astragalar peg distally, which Langer et al. (2000b) homologized with the astragalocalcaneal canal of other basal archosauromorphs. However, this excavation is not as clear in *T. sulcognathus* as in *I. genovefae*. The posterior surface of the astragalus has a well-developed transverse boss spanning from the lateral astragalar peg to the medial region of the articular facet for the centrale. It forms a bar that is unique within Rhynchosauria and represents an autapomorphic trait of *T. sulcognathus*.

Three metapodials are preserved in UFRGS-PV-0298T. One is isolated, whereas the others are partially preserved articulated to phalanges. These share the general morphology of other rhynchosaur metapodials, which are rather alike in the fore- and hind limbs. Yet, they are assumed to represent metacarpals, because only elements of the forelimb are preserved in the specimen, but there is not sufficient information to assign them to specific digits. The elements are flat and elongated, with slightly expanded extremities, especially proximally. The shafts are slightly twisted distally counterclockwise, possessing shallow grooves along the middle of both dorsal and ventral surfaces.

The phalanges of UFRGS-PV-0298T form two digits with at least four elements each, probably two of the digits 3–5. The two isolated phalanges of UFRGS-PV-0232T and the nine of UFRGS-PV-0290T are more robust, and may represent pedal phalanges. The latter specimen has four phalanges forming a complete toe, whereas the remaining ones (including two unguis) are isolated. Despite their size discrepancy, the phalanges attributed to *T. sulcognathus* share the same general morphology. The more compact proximal elements have expanded extremities, proximal ends with biconcave facets, and extend beneath the following phalanx. Collateral depressions are seen on the ginglymoid distal ends, indicating the presence of strong collateral ligaments.

The two unguis phalanges have distinct morphologies. One of them is stouter than the other, modestly curved, and has pointed distal tip, whereas the other is strongly compressed lateromedially. This variation can be attributed to different finger positions, because inner digits are usually more laterally compressed, and outer ones tend to have stouter unguis (Benton, 1983, 1990; Hone and Benton, 2008).

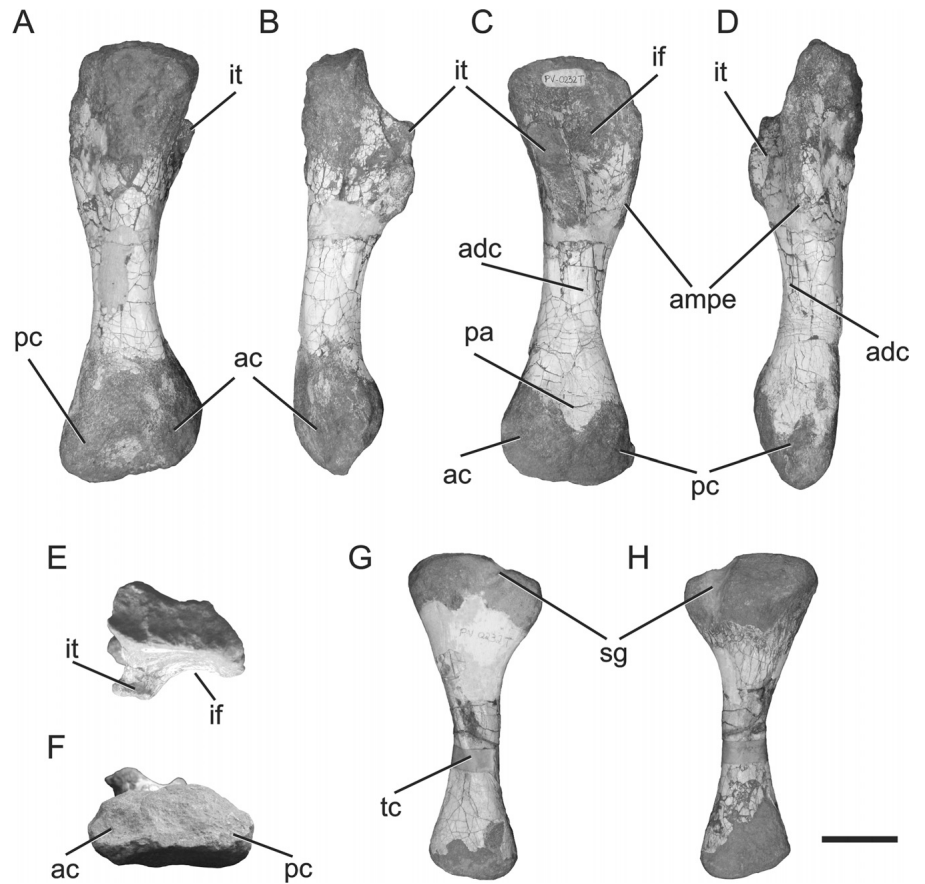


FIGURE 13. *Teyumbaita sulcognathus* (UFRGS-PV-0232). Right femur (A–F) and tibia (G–H). A, dorsal view; B, anterior view; C, ventral view; D, posterior view; E, proximal view; F, distal view; G, medial view; H, lateral view. Scale bar equals 3 cm.

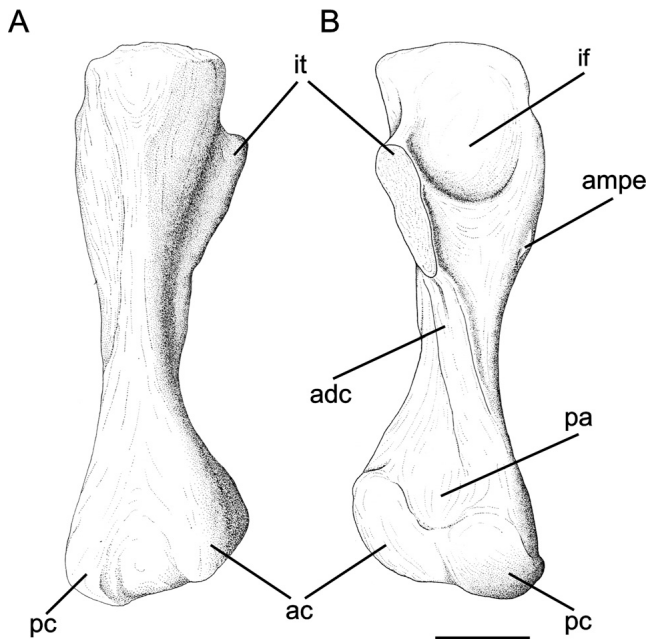


FIGURE 14. *Teyumbaita sulcognathus* (UFRGS-PV-0232T). Schematic drawings of right femur. A, dorsal view; B, ventral view. Modified from Schultz (1986). Scale bar equals 3 cm.

DISCUSSION

In contrast to previous works (Benton, 1983; Langer and Schultz, 2000; Langer et al., 2000b; Montefeltro et al., 2010), the present paper does not support the idea that rhynchosaurs all shared a conservative postcranial morphology. In fact, there are important variations in these elements, including autapomorphic characters that can be added to the diagnosis of *T. sulcognathus*. Characters varying among the three specimens of the taxon (e.g., differences in the axial neural spine morphology, the femur/tibia length ratio, and the origin of the femoral internal trochanter) show that postcranial morphology is also variable intraspecifically. In addition, some characters are potentially useful for phylogenetic analyses, which are tested according to the parameters described below.

Phylogenetic Analysis

Six potentially informative characters were added to the data matrix of Langer et al. (2010) in order to test their effect on rhynchosaur phylogeny (see Appendix 1). The resulting data matrix (Appendix 2 and online Supplemental Data) was analyzed using TNT version 1.1 (Goloboff et al., 2008) using the implicit enumeration algorithm. *M. browni* was constrained as the basal-most taxon and *H. browni* as the sister group of Rhynchosauridae sensu Langer et al. (2010). The latter is formed by eight taxa (see Appendix 3), as in the ‘second analysis’ of Langer et al. (2010).

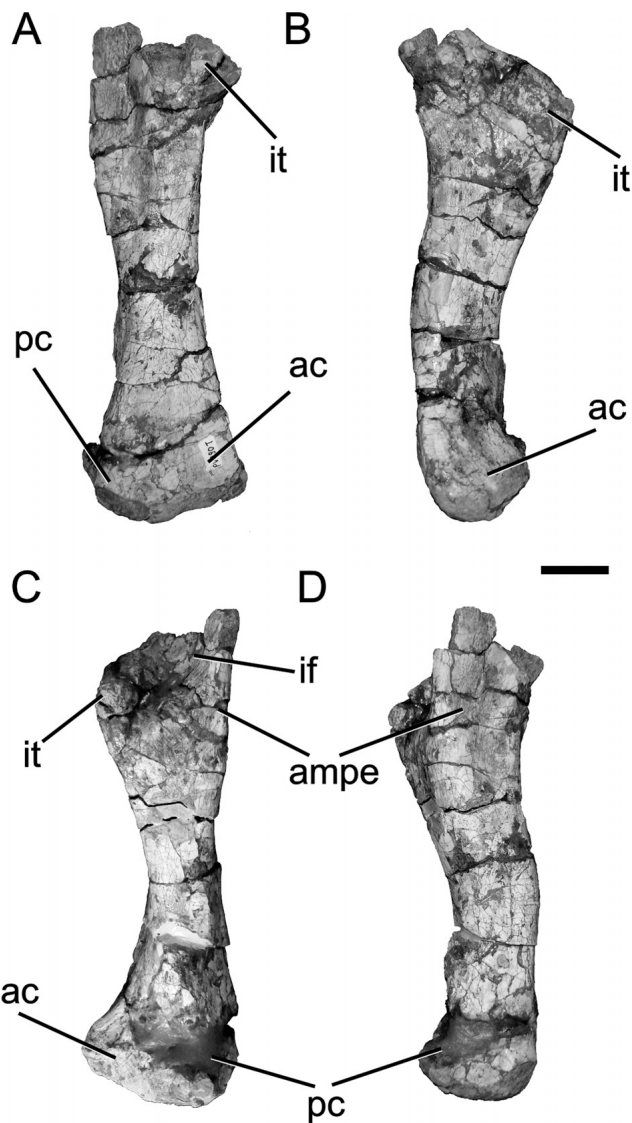


FIGURE 15. *Teyumbaita sulcognathus* (UFRGS-PV-0290T). Right femur. **A**, dorsal view; **B**, anterior view; **C**, ventral view; **D**, ventral view. Scale bar equals 3 cm.

Two most parsimonious trees (MPTs) of 104 steps were recovered, depicting the same structure as that of Langer et al. (2010) (Fig. 19). The only unresolved relationship concerns the position of *Bentonyx sidensis* Langer, Montefeltro, Hone, Whatley, and Schultz, 2010, as the sister taxon of either *Fodonyx spenceri* (Benton, 1990) plus Hyperodapedontinae or *S. stockleyi* plus the 'Mariane rhynchosaur.' The inclusion of the newly proposed postcranial characters did not change the previously recovered topology, but two new rhynchosaurid apomorphies (axis with a ventral keel, crest on the anteromedial region of tibial shaft) as well as two delayed synapomorphies for Hyperodapedontinae (postaxial cervical vertebrae with ventral keel, supinator process formed by a low supinator ridge and the ligament groove) were recognized.

A recently discussed issue in rhynchosaur taxonomy concerns the identification of two different genera in the Anisian-aged

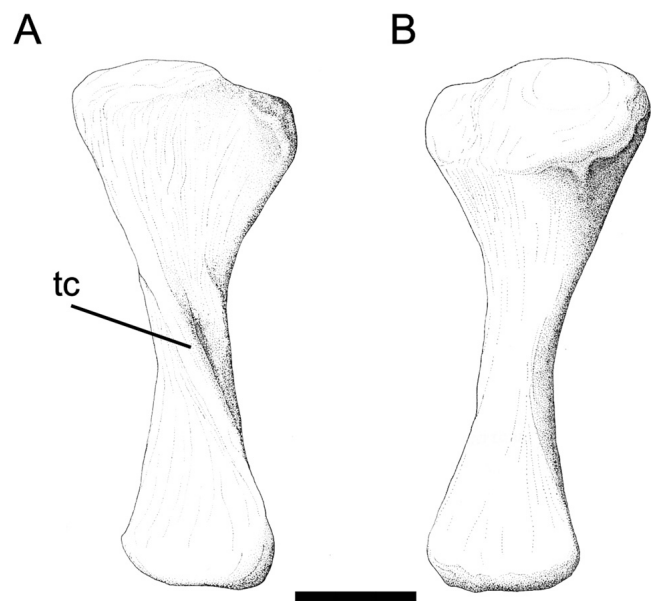


FIGURE 16. *Teyumbaita sulcognathus* (UFRGS-PV-0232T). Schematic drawings of right tibia. **A**, medial view; **B**, lateral view. Modified from Schultz (1986). Scale bar equals 3 cm.

Otter Sandstone Formation of south Devon, England (Hone and Benton, 2008; Langer et al., 2010). The presence of both *F. spenceri* and *B. sidensis* in the same stratigraphic unit precludes an unambiguous referral of the postcranial specimen EX-EMS 79/1992 to either of the genera (Langer et al., 2010). An exploratory analysis was conducted in order to elucidate

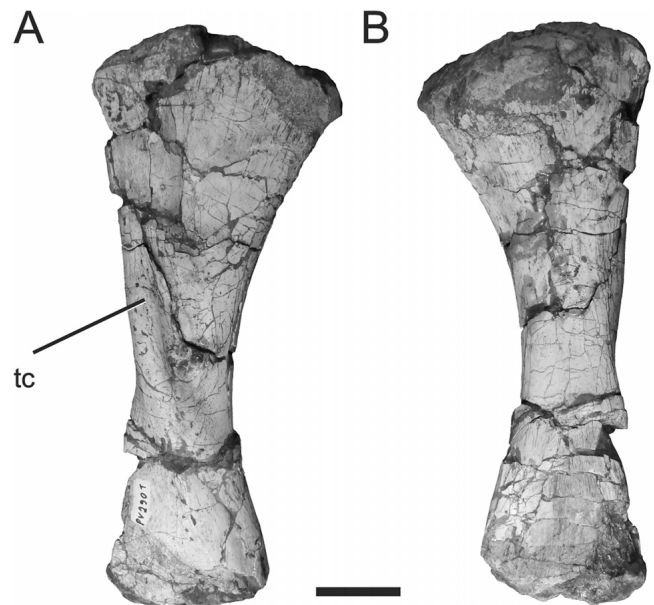


FIGURE 17. *Teyumbaita sulcognathus* (UFRGS-PV-0290T). Right tibia. **A**, medial view; **B**, lateral view. Scale bar equals 3 cm.

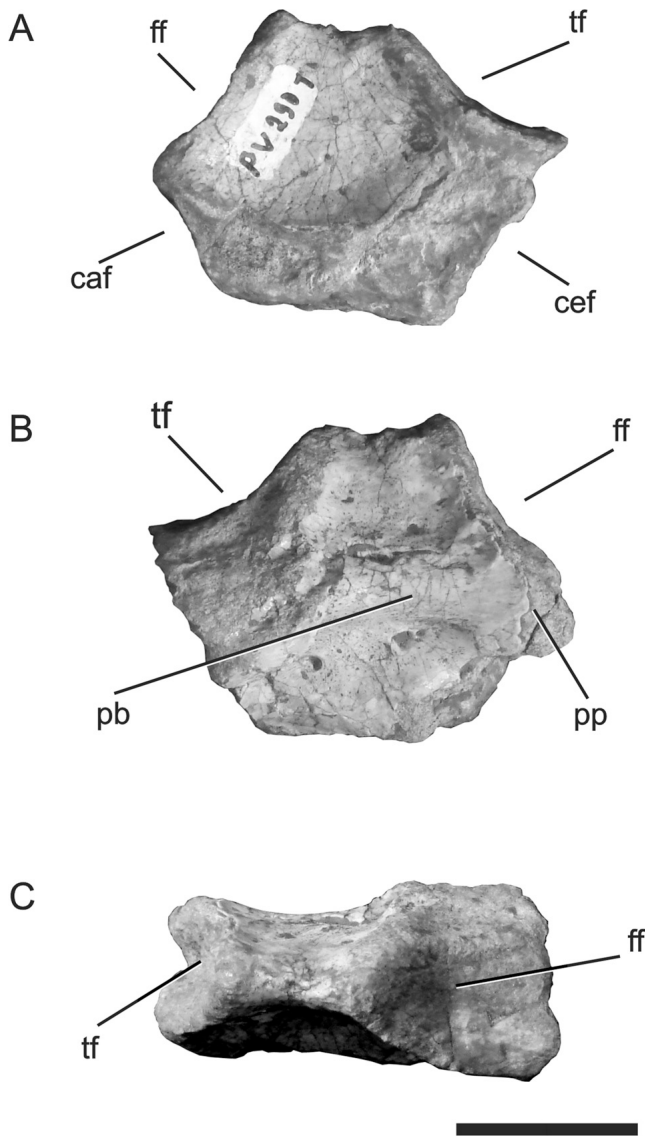


FIGURE 18. *Teyumbaita sulcognathus* (UFRGS-PV-0290T). Right asragalus. **A**, anterior view; **B**, posterior view; **C**, proximal view. Scale bar equals 2 cm.

the affinities of EXEMS 79/1992. It was included as a discrete taxonomic unit in the matrix and the same search protocol was employed. This resulted in 12 MPTs (of 104 steps). The strict consensus tree (Fig. 19) has a less resolved topology, with a highly polytomic Hyperodapedontidae. Yet, when the MPTs are considered separately, a clear pattern emerges. In all trees, EXEMS 79/1992 is placed on the branch leading to Hyperodapedontinae, where it can assume any of the possible positions. In addition, EXEMS 79/1992 is never associated with *B. sidensis*, even in trees in which the latter has a pro-Hyperodapedontinae placement. Only four characters could be scored for EXEMS 79/1992, and clearly further inquiry and more complete specimens are required. Yet, the present results suggest its association with *F. spenceri*, rather than *B. sidensis*.

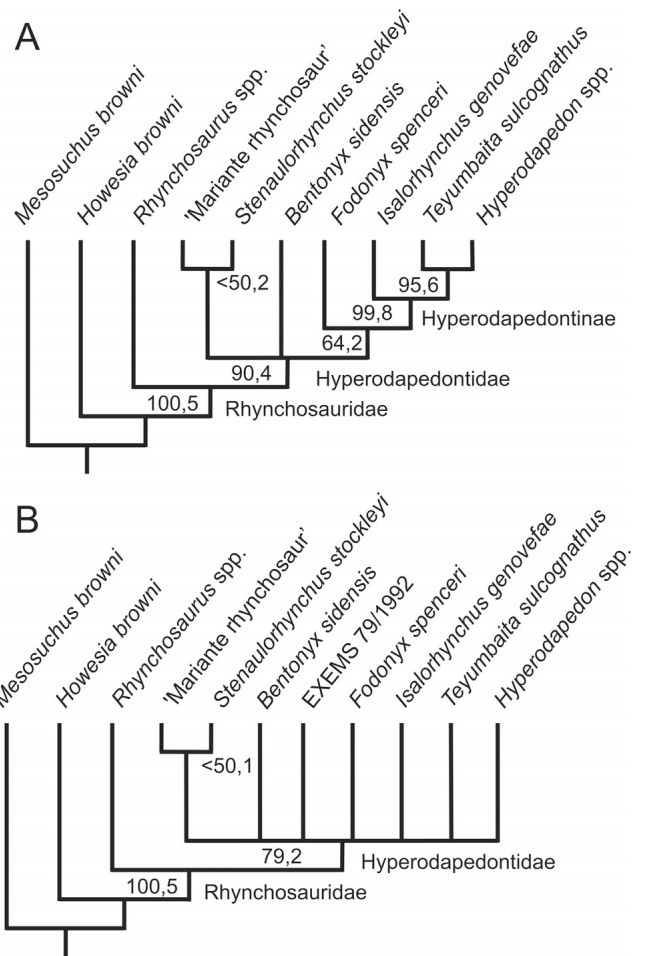


FIGURE 19. Phylogenetic relations of Rhynchosauria. **A**, strict consensus of the two most parsimonious trees (MPTs) recovered in the analysis including six new postcranial characters; **B**, strict consensus of the 12 MPTs recovered in the analysis including EXEMS 79/1992. Bootstrap (1000 replicates) and 'Bremer support' values of each node are indicated. Arrows designate stem-based taxa according to Langer et al. (2010).

CONCLUSIONS

The comparative study presented here reveals that the postcranial morphology of rhynchosaur is not as conservative as thought previously (Benton, 1983; Langer and Schultz, 2000; Langer et al., 2000a; Nesbitt and Whatley, 2004). Different levels of variation were recognized, from intraspecific to those defining rhynchosaur internal relationships. This variation in postcranial morphology offers new information on the phylogenetic relationships of rhynchosaur and emphasizes the importance of considering postcranial data in phylogenetic studies of the group. This corroborates the hyperodapedontine affinity of *T. sulcognathus*, and also suggests referral of the postcranial specimen EXEMS 79/1992 to that lineage, most likely to *F. spenceri*.

ACKNOWLEDGMENTS

The authors thank A. M. Sá Teixeira for the skillful drawings of the holotype and editors H.-L. You and P. Barrett and reviewers D. Hone and M. Benton for handling/reviewing the manuscript. Conselho Nacional de Desenvolvimento Científico e Tecnológico (CNPq) and Programa de Pós-Graduação em

Biologia Comparada, Faculdade de Filosofia Ciências e Letras de Ribeirão Preto, Universidade de São Paulo, supported this research. This contribution used TNT version 1.1, a program made freely available thanks to a subsidy by the Willi Hennig Society.

LITERATURE CITED

- Azevedo, S. A., and C. L. Schultz. 1987. *Scaphonyx sulcognathus* (sp.nov.), um novo rincossaurídeo do neotriássico do Rio Grande do Sul, Brasil; pp. 99–113 in Proceedings of X Congresso Brasileiro de Paleontologia, Rio de Janeiro.
- Baumel, J. J., and L. M. Witmer. 1993. Osteology; pp. 45–132 in J. J. Baumel (ed.), Handbook of Avian Anatomy: Nomina Anatomica Avium. Publications of the Nuttall Ornithological Club, Cambridge, Massachusetts.
- Benton, M. J. 1983. The Triassic reptile *Hyperodapedon* from Elgin: functional morphology and relationships. Philosophical Transactions of the Royal Society of London, Series B 302:605–717.
- Benton, M. J. 1984. The relationships and early evolution of the Diapsida. Symposia of the Zoological Society of London 52:575–596.
- Benton, M. J. 1985. Classification and phylogeny of the diapsid reptiles. Zoological Journal of the Linnean Society 84:97–154.
- Benton, M. J. 1987. The phylogeny of rhynchosaurs (Reptilia, Diapsida), and two new species; pp. 12–17 in P. M. Currie and E. H. Coster (eds.), Fourth Symposium on Mesozoic Terrestrial Ecosystems, Volume 1. Tyrrell Museum of Paleontology, Drumheller.
- Benton, M. J. 1990. The species of *Rhynchosaurus*, a rhynchosaur (Reptilia, Diapsida) from the Middle Triassic of England. Philosophical Transactions of the Royal Society of London, Series B 328:213–306.
- Broom, R. 1906. On the South African diaptosaurian reptile *Howesia*. Proceedings of the Royal Society of London 1906:591–600.
- Buffetaut, E. 1983. *Isalorhynchus genovefae*, n. g. n. sp. (Reptilia, Rhynchocephalia), un nouveau rhynchosaur du Trias de Madagascar. Neues Jahrbuch für Geologie und Paläontologie, Monatshefte 1983:465–480.
- Carroll, R. L. 1976. *Notesuchus*—the oldest known rhynchosaur. Annals of the South African Museum 72:37–57.
- Chatterjee, S. 1969. Rhynchosaurs in time and space. Proceedings of the Geological Society of London 1658:203–208.
- Chatterjee, S. 1974. A rhynchosaur from the Upper Triassic Maleri Formation of India. Philosophical Transactions of the Royal Society of London, Series B 267:209–261.
- Dilkes, D. W. 1995. The rhynchosaur *Howesia browni* from the Lower Triassic of South Africa. Palaeontology 38:665–685.
- Dilkes, D. W. 1998. The Early Triassic rhynchosaur *Mesosuchus browni* and the interrelationships of basal archosauromorph reptiles. Philosophical Transactions of the Royal Society of London, Series B 353:501–541.
- Evans, S. E. 1988. The early history and relationships of the Diapsida; pp. 221–260 in M. J. Benton (ed.), The Phylogeny and Classification of the Tetrapods, Volume 1. Clarendon Press, Oxford.
- Gervais, P. 1859. Zoologie et Paléontologie Française, second edition. Arthus Bertrand, Paris, 544 pp.
- Goloboff, P., J. Farris, and K. Nixon. 2008. TNT, a free program for phylogenetic analysis. Cladistics 24:774–786.
- Haughton, S. H. 1932. On a collection of Karoo vertebrates from Tanganyika territory. Quarterly Journal of the Geological Society of London 88:643–662.
- Hone, D. W. E., and M. J. Benton. 2008. A new genus of rhynchosaur from the Middle Triassic of SW England. Palaeontology 51:95–115.
- Huene, F. v. 1929. Über Rhynchosauries und andere Reptilien aus den Gondwana-ablagerungen Südamerikas. Geologische und Paläontologische Abhandlungen 17:1–61.
- Huene, F. v. 1938. *Stenaulorhynchus*, ein Rhynchosauride der Ostafrikanischen obertias. Nova Acta Leopoldina 6:80–121.
- Huene, F. v. 1942. Die Fossilen Reptilien des Sudamerikanischen Gondwanalandes. C. H. Beck, Munich, 342 pp.
- Hunt, A. P., and S. G. Lucas. 1991. A new rhynchosaur from the Upper Triassic of west Texas, and the biochronology of Late Triassic rhynchosaurs. Palaeontology 34:927–938.
- Huxley, T. H. 1859. Postscript to Murchinson, R. I.. On the sandstones of Morayshire (Elgin &c.) containing reptilian remains, and their relations to the Old Red Sandstone of that country. Quarterly Journal of the Geological Society of London 15:138–152.
- Langer, M. C., and C. L. Schultz. 2000. A new species of the Late Triassic rhynchosaur *Hyperodapedon* from the Santa Maria Formation of South Brazil. Palaeontology 43:633–652.
- Langer, M. C., J. Ferigolo, and C. L. Schultz. 2000a. Heterochrony and tooth evolution in hyperodapedontine rhynchosaurs (Reptilia, Diapsida). Lethaia 33:119–128.
- Langer, M. C., M. Boniface, G. Cuny, and L. Barbieri. 2000b. The phylogenetic position of *Isalorhynchus genovefae*, a Late Triassic rhynchosaur from Madagascar. Annales de Paléontologie 86:101–127.
- Langer, M. C., F. C. Montefeltro, D. W. E. Hone, R. Whatley, and C. L. Schultz. 2010. On *Fodonyx spenceri* and a new rhynchosaur from the Middle Triassic of Devon. Journal of Vertebrate Paleontology 30:1884–1888.
- Long, R. A., and P. A. Murry. 1995. Late Triassic (Carnian and Norian) tetrapods from the southwestern United States. New Mexico Museum of Natural History and Science, Bulletin 4:1–253.
- Lydekker, R. 1885. Reptilia and Amphibia of the Maleri and Denwa Groups. Palaeontologia Indica 4:1–28.
- Montefeltro, F. C., M. C. Langer, and C. L. Schultz. 2010. Cranial anatomy of a new genus of hyperodapedontine rhynchosaur (Diapsida, Archosauromorpha) from the Upper Triassic of Southern Brazil. Earth and Environmental Sciences Transactions of the Royal Society of Edinburgh 101:27–52.
- Nesbitt, S., and R. Whatley. 2004. The first discovery of a rhynchosaur from the Upper Moenkopi Formation (Middle Triassic) of northern Arizona. PaleoBios 24:1–10.
- Osborn, H. F. 1903. The reptilian subclasses Diapsida and Synapsida and the early history of the Diaprosauria. Memoirs of the American Museum of Natural History 1:449–507.
- Owen, R. 1842. Description of an extinct lacertian reptile, *Rhynchosaurus articeps*, Owen, of which the bones and footprints characterize the upper New Red Sandstone at Grinsill, near Shrewsbury. Transactions of the Cambridge Philosophical Society 7:355–369.
- Romer, A. S. 1956. Osteology of the Reptiles. University of Chicago Press, Chicago, Illinois, 772 pp.
- Romer, A. S. 1966. Vertebrate Paleontology. University of Chicago Press, Chicago, Illinois, 468 pp.
- Schultz, C. L. 1986. Osteologia parcial do pós crânio de *Scaphonyx sulcognathus* Azevedo 1982 (Reptilia, Diapsida, Rhynchocephalia). M.S. thesis, Instituto de Geociências, Universidade Federal do Rio Grande do Sul, Porto Alegre, Brazil, 139 pp.
- Schultz, C. L. 1991. Os rincossauros Sul-americanos e suas relações com outros representantes do grupo. Ph.D. dissertation, Instituto de Geociências, Universidade Federal do Rio Grande do Sul, Porto Alegre, Brazil, 416 pp.
- Schultz, C. L., and S. A. Azevedo. 1990. Dados preliminares sobre a ocorrência de uma nova forma de rincossauro para o Triássico do Rio Grande do Sul–Brasil. Paula-Coutiana 4:35–44.
- Sill, W. D. 1970. *Schaphonyx sanjuanensis*, nuevo rincossauro (Reptilia) de la Formación Ischigualasto, Triásico de San Juan, Argentina. Ameghiniana 7:341–354.
- Tupi-Caldas, J. A. L. 1933. Curso Geral de Mineralogia e Geologia, Aplicada ao Brasil. Livraria Globo, Porto Alegre, Brazil, 349 pp.
- Watson, D. M. S. 1912. *Mesosuchus browni*, gen. et spec. nov. Records of the Albany Museum 2:298–299.
- Whatley, R. 2005. Phylogenetic relationship of *Isalorhynchus genovefae*, the rhynchosaur (Reptilia, Archosauromorpha) from Madagascar. Ph.D. dissertation, University of California, Santa Barbara, California, 276 pp.
- Yates, A. M. 2004. *Anchisaurus polyzelus* (Hitchcock): the smallest known sauropod dinosaur and the evolution of gigantism among sauropodomorph dinosaurs. Postilla 230:1–58.

Submitted March 26, 2012; revisions received June 15, 2012; accepted July 1, 2012.

Handling editor: You Hailu.

APPENDIX 1. Character descriptions. The 65 characters used in the phylogenetic analyses are described below (along with the character states). The character–taxon matrix is presented in Appendix 2. Characters 36, 43, and 47 were treated as additive. Characters are either new or adapted from previously published

analyses (acknowledged accordingly). New postcranial characters are at the end of the list (characters 60–65).

- (1) Skull dimensions: longer than broad (0); broader than long (1) (Benton, 1984).
- (2) Skull height: <50% of the midline length (0); >50% of the midline length (Hone and Benton, 2008).
- (3) Orbit orientation: mostly lateral (0); mostly dorsal (1) (Langer and Schultz, 2000).
- (4) Orbital medial margin: rounded (0); forming a marked angle (1) (Montefeltro et al., 2010).
- (5) Jugal and maxillary heights below the orbit ventral margin: maxilla higher (0); jugal higher (1) (Benton, 1984).
- (6) Jugal-lacrimal contact: minimal (0); extensive contact of the jugal anterior process (1) (Whatley, 2005).
- (7) Jugal lateral surface: anguli oris crest does not reach jugal anterior process (0); anguli oris crest reaches jugal anterior process (1) (Benton, 1984).
- (8) Jugal surface dorsal to anguli oris crest: lacking a secondary crest (0); with a secondary anguli oris crest (1) (Langer and Schultz, 2000).
- (9) Lateral overlap of maxilla by jugal: absent or minimally expanded (0); well developed (1) (Whatley, 2005).
- (10) Jugal subtemporal process: height >50% of the length (0); height <50% of the length (1) (Dilkes, 1995).
- (11) Relative widths of postorbital bar and lower temporal fenestra: <0.4 (0); >0.4 (1) (Langer and Schultz, 2000).
- (12) Dorsomedial surface of prefrontal near the orbital rim: flat or slightly concave (0); deeply concave (1) (Whatley, 2005).
- (13) Procumbent lacrimal and prefrontal anterolateral margin: absent (0); present (1) (Whatley, 2005).
- (14) Dorsal groove on frontal: deeper posteriorly (0); same depth throughout its length (1) (Dilkes, 1995).
- (15) Well-marked 'V'-shaped crest along frontal-postfrontal contact: absent (0); present (1) (Montefeltro et al., 2010).
- (16) Frontal and parietal midline lengths: frontal longer (0); parietal longer (1) (Benton, 1987).
- (17) Postfrontal: excluded from upper temporal fenestra border (0); forming the upper temporal fenestra border (1) (Dilkes, 1998).
- (18) Postfrontal dorsal surface: flat (0); markedly concave (1) (Dilkes, 1995).
- (19) Postorbital anteroventral process: expanding ventral to the level of the orbital midpoint (0); expanding dorsally to orbital height midpoint (1) (Dilkes, 1998).
- (20) Postorbital ventral process: expands anterior to the jugal (0); fits dorsal to the jugal (1) (Whatley, 2005).
- (21) Postorbital-parietal suture: visible in dorsal view (0); hidden in dorsal view (1) (Dilkes, 1998).
- (22) Parietal body: not expanded laterally at midlength (0); expanded laterally at midlength (1) (Montefeltro et al., 2010).
- (23) Parietal transverse process: posterolaterally directed (0); laterally directed (1) (Montefeltro et al., 2010).
- (24) Distal tip of parietal transverse process: not anteriorly curved (0); anteriorly curved (1) (Montefeltro et al., 2010).
- (25) Squamosal ventral process: thinner than 50% of dorsoventral length (0); broader than over 50% of dorsoventral length (1) (Benton, 1990).
- (26) Relative position of quadratojugal and squamosal processes: squamosal ventral process anterior to quadratojugal dorsal process (0); squamosal ventral process overlapping the quadratojugal dorsal process (1) (Whatley, 2005).
- (27) Supratemporal: present (1); absent (1) (Benton, 1984).
- (28) Ventral margin of opisthotic paroccipital process: convex (0); straight (1) (Montefeltro et al., 2010).
- (29) Pterygoid midline suture length: greater than or equal to the distance between the posterior margin of the suture and the basiptyergoid articulation (0); less than the distance between the posterior margin of the suture and the basiptyergoid articulation (1) (Whatley, 2005).
- (30) Elements forming the border of the suborbital fenestra: ectopterygoid, palatine, and maxilla (0); ectopterygoid and palatine only (1) (Dilkes, 1995).
- (31) Occipital condyle position: anterior to craniomandibular articulation (0); aligned to craniomandibular articulation (1) (Benton, 1984).
- (32) Basisoccipital and basisphenoid/parasphenoid lengths: basisphenoid/parasphenoid longer (0); basisoccipital longer (1) (Langer and Schultz, 2000).
- (33) Relative positions of the basiptyergoid process of the basisphenoid and the ectopterygoid process of the pterygoid: at the same level (0), basiptyergoid process of the basisphenoid posterior to ectopterygoid process of the pterygoid (1) (Dilkes, 1995).
- (34) Basiptyergoid process dimensions (dorsoventral length, anteroposterior width): longer than wide (0); wider than long (1) (Langer and Schultz, 2000).
- (35) Mandible depth: <0.25 of the total length (0); >0.25 of the total length (1) (Benton, 1984).
- (36) Dentary length: half, or less, than the total mandibular length (0); greater than half of the total mandibular length (1) (Benton, 1990).
- (37) Medial maxillary groove: absent (0); present but not reaching the anterior half of the maxilla (1); present and reaching the anterior half of the maxilla (2) (Benton, 1984).
- (38) Maxillary area lateral to main groove: narrower than the medial area (0); same width or broader than the medial area (1) (Benton, 1990).
- (39) Maxillary cross-section lateral to main groove: crest-shaped (0); cushion-shaped (1) (Langer et al., 2000b).
- (40) Tooth rows lateral to main maxillary groove: a single clear row (0); more than one clear row (1) (Langer and Schultz, 2000).
- (41) Number of tooth rows medial to main maxillary groove: two rows and scattered teeth (0); three or more tooth rows (1) (Langer et al., 2000b).
- (42) Occlusal tooth rows on the anterior half of the maxilla: four or more tooth rows (0); fewer than four tooth rows (1) (Whatley, 2005).
- (43) Maxillary lingual teeth: absent (0); scattered teeth (1); large number of teeth on the medial surface of the bone (2) (Benton, 1984).
- (44) Maxillary teeth: only conicals (0); conicals and 'pyramidal' (1) (Whatley, 2005).
- (45) Dentary teeth: only conicals (0); conical and anteroposteriorly compressed (1) (Whatley, 2005).
- (46) Posterior-most dentary teeth: on the anterior half of dentary (0); on the posterior half of dentary (1) (Langer and Schultz, 2000).
- (47) Lingual dentary teeth: absent (0); present and forming one row (1); present and forming more than one row (2) (Benton, 1984).
- (48) Dentary teeth on the dentary lingual surface: scattered (0); crowded (1) (Benton, 1985).
- (49) Truncal vertebrae with ossified intercentrum: present (0); absent (1) (Evans, 1988).
- (50) Epiphyses on cervical postzygapophyses: spine-shaped (0); crest-shaped (1) (Whatley, 2005).
- (51) Second sacral vertebra: with a notch between the iliac articular surface and the posterior process (0); posterior process continuous to the iliac articular surface (1) (Dilkes, 1998).
- (52) Caudal vertebrae neural spines: height twice the length (0); height less than twice the length (1) (Dilkes, 1998).
- (53) Interclavicle: posterior process longer than twice the lateral processes (0); posterior process shorter than twice the lateral process (1) (Dilkes, 1998).

- (54) Posterior process of the coracoid: present (0); absent (1) (Benton, 1984).
- (55) Dorsal margin of the ilium: anterior process <15% of the length of the posterior process (0); anterior process >15% of the length of the posterior process (1) (Dilkes, 1995).
- (56) Pubic tubercle: present (0); absent (1) (Whatley, 2005).
- (57) Internal trochanter: continuous with the femoral head (0); separated from femoral head (1) (Whatley, 2005).
- (58) Relative size of astragalar articular facets: tibial facet greater than centrale facet (0); centrale facet greater than tibial facet (1) (Langer and Schultz, 2000).
- (59) Metatarsal I: longer than broad (0); broader than long (1) (Hone and Benton, 2008).
- (60) Axis ventral keel: present (0); absent (1).
- (61) Axial parapophysis: present (0); absent (1).
- (62) Cervical postaxial vertebrae ventral keel: absent (0); present (1).
- (63) Position of the transverse process of cranial truncal vertebrae: at the level of prezygapophysis (0); posteriorly located in the vertebra centrum (1).
- (64) Supinator process on the external surface of humeral ectepicondyle: absent (0); present and hook-shaped (1); present and formed by a low supinator ridge and ligament groove (2).
- (65) Crest on anteromedial region of tibial shaft: absent (0); present (1).

APPENDIX 2. Character-state matrix. Missing data are marked as '?', nonapplicable characters as '-', and variable condition under '['].

Mesosuchus browni
 000000--0-10000001000000000010000000-----000
 00000000000000000000

Howesia browni
 00000?-0--100010010000000??00100000??-----0100
 00?0?00??010000?00

Rhynchosaurus spp.
 0000000001000001000000000000?0000001000001100?
 20??00000?001101?

Stenaulorhynchus stockleyi
 000110000?010111001001010000110000002000112000
 2100010011001100001

'Mariante rhynchosaur'
 0100100000010111110010110001000100??200011200?
 21????????????110??

Bentonyx sidensis
 000111000?01001010001110??01110010????0??1???
 20????????????????

Fodonyx spenceri
 11??1?000????????????????00??1????011010011000
 21????????????????

EXEMS 79/1992
 ???
 ??1?????????1??0?

Isalorhynchus genovefae
 111?1111111010????00??1?11?0011100110110010111
 101011111111??102

T. sulcognathus
 11111111011100111111101110011101112001101111
 2111??1??1??00112

Hyperodapedon spp.
 111011101 [01] [01] 11011011 [01] 110111 [01] [01] 111
 [01] 111] 01] [01] 1110 [01] 111 [012] 011111110 [01] 11
 1 [01] 102

APPENDIX 3. Operational taxonomic units. Ingroup and outgroup operational taxonomic units used in the phylogenetic analysis. Sources of data for coding are listed for each taxon (specimens studied firsthand and published descriptive accounts).

Outgroup

Mesosuchus browni Watson, 1912 (SAM-PK-K5882, SAM-PK-K6536, SAM-PK-K7416, SAM PK-K7701; Dilkes, 1998).
Howesia browni Broom, 1906 (SAM-PK-K5884, SAM-PK-K5885, SAM-PK-K5886; Dilkes, 1995).

Ingroup

Rhynchosaurus spp.—*R. articeps* Owen, 1842, and *R. brodiei* Benton, 1990 (SHRBM G-132/1982, NHMUK R1236, NHMUK R1237, NHMUK R8495; Benton, 1990).
Stenaulorhynchus stockleyi Haughton, 1932 (IGMPT-317; Huene, 1938).
 'Mariante rhynchosaur'—Taxon not formally described; see Schultz and Azevedo (1990) (UFRGS-PV-0168T, UFRGS-PV-0315T).
Bentonyx sidensis Langer, Montefeltro, Hone, Whatley, and Schultz, 2010 (BRSUG 27200; Hone and Benton, 2008; Langer et al., 2010).
Fodonyx spenceri (Benton, 1990) (EXEMS 60/1985.292; Benton, 1990).
Isalorhynchus genovefae Buffetaut, 1983 (Whatley, 2005).
Hyperodapedon spp.—*H. gordonii* Huxley, 1859; *H. huxleyi* Lydekker, 1885; *H. mariensis* (Tupi Caldas, 1933); *H. sanjuanensis* (Sill, 1970); *H. huenei* Langer and Schultz, 2000 (NHMUK R699, NHMUK G281 FZB-PV-1867, MACN-18185, UFRGS-0132; Sill, 1970; Chatterjee, 1974; Benton, 1983; Langer and Schultz, 2000).
Teyumbaita sulcognathus (Azevedo and Schultz, 1987) (UFRGS-PV-0232T, UFRGS-PV-0298T, and UFRGS-PV-0290T; Montefeltro et al., 2010).
 EXEMS 79/1992—Undetermined taxonomic affinity (Hone and Benton, 2008).